Sjoberg et al.
"Intraseasonal to interannual variability of Kelvin wave momentum fluxes as derived from high-resolution radiosonde data"
ACP-2016-1088

We want to thank both the reviewers for their helpful comments, suggestions, and corrections to the manuscript. We feel that the draft is greatly improved as a result of all of these and hope that it more thoroughly presents our analysis and more precisely explains the results. Due to the great detail of the reviewer responses, the manuscript has undergone a major revision. As such, we would like to first describe and explain the large changes we have made.

Thanks to comment 3 from Reviewer #1, the number of valid data points have been increased. Selection of the sign of omega allows us ensure that k remains positive. None of the results – most importantly, the raw time series – showed that making this change produces unphysical or unexpected results, except in regions where the horizontal wavelength is less than 100 km. In these regions, there are likely spurious oscillations of the sign of our estimated momentum flux. Furthermore, it is not clear that the waves in these regions are truly Kelvin waves given that at 100 km length scales, Kelvin waves are indistinguishable from gravity waves. As a result, we increased the length constraint to 500 km and this removed most of the oscillatory values, while leaving more resolved points within strong easterlies.

Naturally, this methodological change alters many details of our results. For instance, the composite structures change considerably. In the case of the QBO composite, these changes result in a composite structure that even more closely matches expectations and removes the problem that including wave periods between 5-8 days produces missing values in the composite. This latter improvement addresses a comment by Reviewer #2 about excluding those periods from the rest of our analysis.

In the case of the annual cycle composite, the changes are perhaps more noticable, particularly those for zonal wind in the top left panel. We note that, for the annual mean composite, we only include points in the composite where the momentum flux is not a missing value. This is true for each field, not just momentum flux itself. In the previous submission, because many missing values were located in the easterlies, the composite zonal wind structure came from points that were primarily in QBO westerlies or during transition periods. Now that we include additional data points from the QBO easterlies, this brings about the differences in the composite structure.

The suggestion by Reviewer #2 that, before attempting to make the link between the MJO and momentum flux, we first analyze the expected relationship between convection and Kelvin waves also produced a substantive change to the manuscript. The details of this are now included in the Discussion section – separated from the Summary as per a comment by Reviewer #2 – but we can give an overview here.

We determined an appropriate definition for the occurrence of a convective 'event' upstream of the sounding sites and performed composite analysis about these events. This shows that organized convective events precede a positive signal in lower stratospheric momentum flux, as expected. By then comparing those convective events with strong and weak associations to the MJO, we find that the strongly associated events have considerably more flux. This provides a more definite suggestion that the MJO influences stratospheric momentum flux. We believe that a key shortcoming to our previous analysis of this was that we did not require a convective signal (i.e., a forcing mechanism) to be present near the sounding site.

We have addressed your individual comments below in blue.

Reviewer #1

1. In section 2.2, the authors describe in detail the estimation method which is extended from the method used in previous studies. I suggest clarifying the difference, extension, or improvement from the previous method. For example, in P5 L28–31, the authors state that the results from their method are similar to those from previous studies in terms of overall range of vertical wavelengths, confirming the fidelity of the method. However, it is not clearly stated what the improvement/advantage of the present method is. Clarifying this in section 2.2 and/or in conclusion section could help readers and strengthen the paper.

R: Thank you for this comment. We were not clear enough about what is different from prior studies. Our primary difference is just that we use overlapping windows, here overlapping by all but 1 day from the ones prior to or following a given window. This technique of short-time Fourier transform allows for greater temporal resolution of which previous studies, to our knowledge, have not taken advantage. We have added a few sentences to the end of section 2.2 and to the summary in order to clarify this to the reader.

2. P4 L20–23: To demonstrate resolution effects more completely, the sensitivity of estimates not only to output resolutions (Δt_{win} and Δz_{win}) but also to raw data resolutions (i.e., vertical/temporal stepping of raw data before interpolation procedure) could be investigated. For example, from a 50-m resolution profile, one could make a 300-m resolution profile by picking one data point every six points. Interpolation using the original 50-m data and that using the sub-sampled 300-m data can result in different estimates of parameters even for the same Δz_{win} value.

R: we have performed this analysis and not found the results to be different. As an example, the figures below show the comparison of our (left) original 250 m data and 250 m data computed using input data with at least 300 m stepping and (right) the same but for 500 m

resolution and stepping. These two data sets have a linear correlation coefficient of 0.945 and 0.881, respectively. This seems to indicate that there is not high sensitivity to the resolution of the input data, and that changes to the resolution of the input data do not systematically alter the resulting momentum flux estimates.

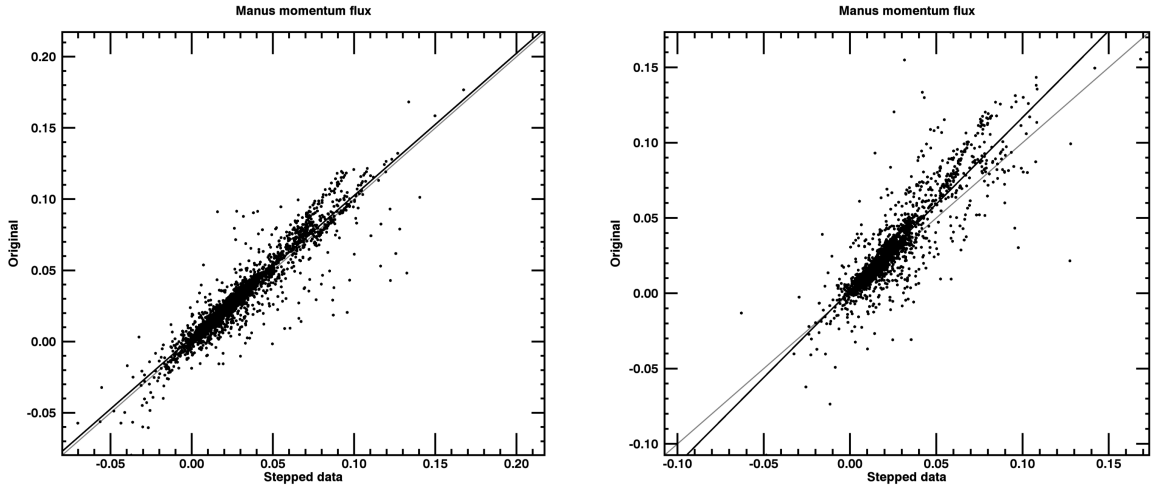

3. P6 L6: "strong easterlies often result in negative k." : This can be in part due to the restriction of ground-based frequency to be positive. In principle, the spectral transform in time just gives the absolute value of the frequency, so that we still have freedom to determine its sign, while the intrinsic frequency (and k) is fixed to be positive. What will happen in the results if negative ground-based frequencies are allowed in the strong easterly regions?

R: Thank you for this insight. We overlooked the possibility of applying this freedom afforded by spectral symmetry. We have discussed this change in our summary above, and made appropriate changes to the text.

4. Figs. 4 and 5: Too many regions are filled by missing for the easterly wind where the Kelvin wave flux is actually maximal (e.g., Ern and Preusse, 2009). Also, the regions of large momentum flux in the westerly shear layer, which are important for the QBO to descend, are very close to the missing regions below. Therefore, the large Kelvin wave flux in such strong easterly regions could be of interest. It would be very nice if the authors explore ways to estimate the momentum flux in such easterly regions, as much as they can.

R: We agree that the fluxes in these regions are of interest. Our original response would have been to discuss that inclusion of additional radiosonde sites in a merged analysis would allow for independent estimation of the zonal wavelengths. This independent estimation could reduce the frequency of negative values of k in regions of strong easterlies/westerly shear, allowing our method to then estimate the momentum flux there. While we think that this is a

worthwhile procedure for future analysis, addressing your previous comment helped to greatly reduce the number of missing values.

5. I feel that the grammar used is not perfect. The judgment for English editing will be left to the authors and other reviewers.

R: we have performed a thorough reading of the text, paying particular attention to improving grammar and sentence structures.

P1 L4-5: "Estimates . . . larger." : Readers could read this as the authors themselves also estimated the momentum flux from satellite and reanalysis data. I suggest deleting this sentence.

R: deleted.

P2 L5: "identical" → "opposite" ? Please check this and make it consistent with the descriptions in this paragraph.

R: this was overlooked, but is now changed to be correct.

P2 L8–17: Some phrases are repetitive within this paragraph. Please reorganize this paragraph.

R: we have edited the text somewhat in this paragraph, but retained most of it because we feel that a thorough explanation is worthwhile here.

P2 L19: "vertical momentum" → "zonal momentum"

R: changed.

P3 L9: I suggest including ", variability, " between "climatologies" and "vertical ...", considering the title of this paper.

R: this is a very welcome suggestion. Changed.

P3 L16: What do the "two climatologies" mean?

R: we mean the climatological annual cycle and the QBO mean cycle. We have made this more clear at this point, and changed the title of section 5 (to "Annual cycle and the QBO") for more clarity.

P3 L29: What is an approximated vertical step corresponding to the 2 seconds, considering lifting speed of the balloon?

R: on average, about 10 m. We have put this approximate value in the text.

P4 L13: "linearly interpolated in height and spline interpolated in time": The linear interpolation also is one of the spline interpolations. Please include the order of the spline interpolation in time used here (e.g., cubic spline).

R: thank you for this clarification. We have corrected the text.

P4 L17: "linear and spline" → "orders of" / "changes to" → "changes in"

R: changed.

P4 L18: "point. An exception to this is if the time" → "point, unless the time"

R: we feel that this would create a run-on sentence. We have altered the sentence in a way that we hope is clearer.

P4 footnote: "too short" → "too long" ? Based on my experience, the scale height in the tropical lower stratosphere is about 6 km or even shorter.

R: we have made this change.

P5 L6: "but that variations in the stratification ... L_z." : Where (and how) is this assumption used in your method ?

R: this is the WKBJ assumption. It was used in the derivation of Eqs. (1)-(4), principally through the wavelike approximations made for each geophysical field. We added more discussion about the use of this assumption to the text.

P5 L25: “temperature leads zonal wind”: What is the criterion for this lead/lag relation ? e.g., phase difference of 45–135°, or 0–180° ? It is better to include this information in the text, considering that the determination of lead/lag relation between two variables is ambiguous as the phase difference becomes close to 0 or 180°.

R: we have previously tested the difference between these two criteria and found the results to not be significantly different. However, you make an excellent point that we should err on the side of certainty in this lead/lag relation. We have updated our method and included this information in the text.

P5 L27: Please include the minus sign in front of the “2π”, as the authors defined m to be negative (P5 L5).

R: done.

Fig. 1 caption: Please include “40-day mean” in (c) in front of “vertical quadrature spectrum”. In addition, I suggest changing “filtering window” to “period” (L5; L6; L8) in order to clarify its meaning.

R: we have made these changes.

P8 L6: “as expected ... (a)” : Zonal wavelengths cannot be expected from visual inspection of (a) in which the time–height cross section is shown.

R: indeed. We have made this change.

Fig. 2: The right axes are not linear while the left axes are linear. I have thought that the percent difference is defined as $(M - M_0)/M_0$ where M_0 is the momentum flux estimated with the reference (250-m and 24-hour) resolutions. If it is right, the percent difference and M have linear relationship.

R: Percent difference, to our knowledge, is defined as (M-M0)/ ((M+M0)/2), while percent error is defined in the way you stated.

Fig. 2 caption: “time mean momentum fluxes from ...” : Based on the text, it is more precise to describe this as “momentum flux, estimated using time-mean parameters, from ...”

R: we agree with this correction, but the method of calculating the momentum flux for this experiment has changed to instead use the daily values of the parameters and then calculate the time mean.

P9 L7–10: As already pointed out by the technical review of the manuscript, there is no curve in the figure that the authors describe in these sentences. The dashed curve, which is referred to by these sentences, is totally different one, as mentioned in the figure caption and on P9 L5.

R: thank you for noticing this. It has been removed.

P9 L18: "enhanced" : What does this mean ?

R: it is more clear to say "positive" so the text now uses this instead of "enhanced."

P10 L5: "full zonal mean" : I do not agree to use the term "zonal mean momentum flux" for the flux estimated using one-site data, as here. The temporal mean could approximate the zonal mean for zonal wind or temperature in the stratosphere, as mentioned by the authors, but it could not approximate the zonal mean of anomaly flux in general. Please consider revising this, as well as in P17 L13–14.

R: while the derivation of Eqs. (1)-(4) are for the zonal mean momentum flux, we acknowledge that it may be misleading to call our single-site estimates of the flux a true zonal mean. It's not clear (and we have not shown) how these long-term estimates vary along longitude, other than for an additional site located 20 degrees downstream. We have removed the wording as you suggested.

Fig. 6: Could you explain why the parameters in (b)–(d) are weighted by period ? (i.e., reason why the parameters with longer periods are more highlighted)

R: considering it now, this does not seem to be a sensible thing to do. Since panels (c) and (d) are not much different for a simple mean over all wave periods when compared to the period-weighted mean, we elect to do the former in the manuscript.

P14 L1: "the westerly QBO phase persists longer in the lower stratosphere" : This could be partly due to the missing when the wind is easterly. Or, is the zonal mean zonal wind here composited regardless of the missing for momentum flux estimates?

R: this is precisely the reason. Now, with more included points going into the annual mean of the zonal wind (because more momentum flux points are not missing), there is a much larger signal of the QBO easterlies. While it's still true that the westerly phase persists longer over our data record (see Figs. 3 and 4), the easterly winds are stronger. The text now reflects this.

P15 L12: For given zonal mean N and U, the sign of k (i.e., missing or not) depends only on the magnitude of m by Eq. (4), as the authors fix ω to be positive. Thus, the numerous missing for the 5–8 day period bands may imply that for these short periods the vertical wavelengths are shorter than those for 8–20 day waves. Is this true overall? It seems to be not the case for the example in Fig. 1.

R: this is not true overall. There is no forced or implied dependence of vertical wavelengths on wave periods, though this tends to be generally true as can be seen in Fig. 2b. Note though that, in the mean, the 20 day waves have shorter scales than 13.3 day waves.

Fig. 7: While the climatological momentum flux is much larger below 20 km than above as shown in Fig. 6a, the flux below 20 km shown in Fig. 7 seems not that large compared to above, even when averaged over the QBO phases. Does this imply that a large portion of the flux below 20 km shown in Fig. 6a comes from the 5–8 day waves that are excluded in Fig. 7?

R: while this particular issue has been removed from the manuscript, we can inform you that, in the annual mean, these waves periods account for approximately 45-55% of the total momentum flux between 18 and 20 km.

P15 L13: "The same structure" : same as what ?

R: removed, so no longer applicable. Referred to the 5-20 day and the 8-20 day QBO composite having the same structure.

P15 L18–P16 L1: "signals of downward descending fluxes" → "descending signals of the flux"

R: changed.

Fig. 8: Based on the positions of number of days indicated in this figure and based on the shape of the contours in Fig. 7, I assume that the QBO phase bins are centered at 0, 0.25, 0.5, 0.75, and so on. However, the histogram in Fig. 8 is centered at 0.125, 0.375, and so on. Please correct the figure.

R: Fig. 7 should be centered at the half steps 0.124, 0.375, etc. This is now corrected.

P16 L13: “for linear . . . resolution” → “with increased vertical step”

R: changed.

P16 L17: Please insert “for westerly background wind” after “results in larger momentum fluxes”, because there is the inverse relationship for easterly cases (Eq. (4)).

R: we agree that this clarification should be included, and have amended the text. We also briefly discuss that the opposite is true, as this is important for the relation between Kelvin waves and the QBO.

P17 L24: “planetary-scale, zonal mean momentum fluxes” → “planetary-scale wave momentum fluxes”

R: amended.

P18 L5: “MJO is” → something like “active-MJO mean is”

R: no longer included.

P19 L7: “As shown by Fig. 9” → “As mentioned” (It was “not shown”).

R: no longer included.

Reviewer #2

1a) Fig. 1: please consider at a panel of background wind contours so we know what the background wind looks like, and more importantly, we can see whether its varying slowly vertically.

R: Ensuring that WKBJ holds is an important aspect of this work, else our wave-like assumptions do not hold. In this case, the winds are slowly varying during this time span, as can be seen in Fig. 3. Because the winds are displayed there, we opt not to include an additional panel, but have added a note to the reader that they may see the wind over this data window in Fig. 3.

2a) Fig. 2: add the errorbar for each line for each resolution you picked to construct the lines.

Since I'm not clear how many soundings were used, if only a few, you need to explain how robust Fig. 2's results are to a large sample; if a lot of the soundings were used, you can comfortably plot the errorbars out.

R: we first took the time mean of each of the input fields to Eqs. (1) and (3). Doing so allows for very quick calculation of the momentum fluxes for our experiments holding certain input fields constant (e.g. vertical wavelength in Fig. 2). Since we first took the time mean, this obviously did not allow for any type of error analysis. We reformulated this portion of the analysis to instead calculate the momentum flux first, allowing us to then calculate standard errors. Note that this methodological change, along with changes arising from allowance of negative k values, results in changes to the overall amplitude of our results. From the standard error bars, it should be more apparent that the differences between 250 m and 2000 m resolution are significant. We have added text describing this.

3a) Fig. 3: add the explanation of the bold grey line (zero wind line) or add the label in the figure.

R: thank you for noticing this. We have corrected it here and elsewhere.

4a) P13, L4: it would be much straightforward if you can show a scatterplot of your comparison between the two datasets.

R: we don't feel that this substantively adds to the paper enough to justify a figure in the manuscript, but have made clear that the linear correlations between all points 18-25 km are high (0.94). We include the scatterplot below for your consideration, however (units mPa; gray is 1-to-1; black is linear fit).

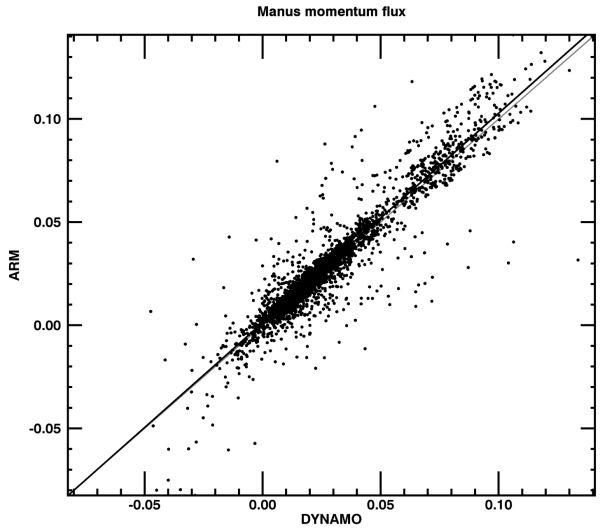

5a) Fig. 7: since you stated that 8-20day Kelvin waves are representative of the total KWMF features of 5-20 day Kelvin waves, and there are a lot of missing data for 5-8 day Kelvin waves using your technique, why not revised Fig. 3, 4, 5, 6 with the 8-20 day Kelvin waves? I think it's very important to keep consistency throughout the paper of the variables you present. Otherwise, you don't know whether the differences are caused by other mechanisms or simply by the inconsistency. Move your explanation of P15, L11-15 to the second paragraph of Section 4.

R: We agree that consistency is vital for proper comparison. Due to changes to method – allowing of negative wave periods in the calculation of k – this is no longer necessary. Kelvin waves with periods between 5-8 days now have a sufficiently large number of valid points to not result in missing values in the QBO composite.

6a) It's very awkward to further extend your discussion about MJO's impact on KWMF in the conclusion section. Why not move this discussion to a subsection of Section 5 (also change the title of Section 5)?

R: with the changes to this analysis, we definitely agree. We have broken out the discussion section (focusing on the relation between convection/MJO and momentum flux) from the summary.

7a) You mentioned you used two indices to indicate the phase of MJO: RMM and OMI. Firstly, you need to clarify which datasets are used to construct these two indices; secondly, you don't even used RMM throughout the paper, if I didn't read too fast to miss that point. Please point the

sentences about RMM out in the MJO section.

R: we did mention that results are not qualitatively different, but this is not really sufficient for including it here. We have removed mentions of the RMM. We also provided more details about the OMI data we use.

8a) Fig. 9: I don't understand the meaning of the x-axis of Fig. 9b. Can't imaging the errorbar could be uniform throughout the layer. Can you add your spread (2*sigma or 3*sigma) to Fig. 9a for both solid and dashed lines (since you have a lot of sounding profiles to composite each of the line), so it would be much more straightforward to check whether they are statistically different.

R: this figure has been removed.

1) How good is your assumption that the vertical wavenumber is constant for a given window of data? My understanding is that you still estimate the vertical wavenumber for each period of Kelvin wave (5-20 days) separately, is that correct? How to justify the impact if it is not the case? Can you assess how many cases in terms of percentage of total that violates the slow-varying-zonal-wind rule (is this the WKB assumption by the way)?

R: the WKBJ approach has been used to derive the equations (1)-(4). As is typically the case, real data does not fit as well as would be liked to the approximations made by this theory. Nevertheless, ensuring that it holds to first order can still yield insight we would not otherwise be able to get (see Andrews et al. 1987, sec. 4.7.4). This condition of slowly-varying zonal wind is one of the assumptions used by the WKBJ approach.

We can estimate how often this assumption is satisfied by first finding the appropriate scales of zonal wind variations. To find the length (time) scale, we take the 1-sigma value of zonal wind (15 m/s) and divide by the local vertical (temporal) derivative. To first order, "slowly varying" is satisfied where these scales are larger than the longest vertical or time scales we consider (15 km or 20 days). These conditions are satisfied in time and space for 99.9% and 85.5% of points, respectively.

As discussed in the aforementioned section by Andrews et al., WKBJ theory has been successfully applied to problems which have not entirely satisfied the assumptions. And, since we find good agreement between our and other authors' work, we feel justified in using these methods despite their shortcomings. If there were glaring unphysical results in our KWMF data, we would be much more cautious about interpretation and utilization of our results. Most features are quite reasonable, however.

Further, these shortcomings motivated us to not focus on specific events, but to instead perform more climatological/composite analysis. By performing our analyses only over a large number of events/cycles, unphysical estimates from where the applied model is invalid should get wiped out. While this is not true in the case of the QBO composite (with only 4 full events entering into it), the high number of points averaged in each bin raises our confidence in it.

We have added additional comments about the usage of WKBJ and our confidence in the results.

2) Please add a sentence or two to clarify that eastward propagating gravity waves (GWs) would not be included in your KWMF calculation, as you only constrain your horizontal wavelength to be > 100 km, fairly fall in the spectrum of internal and inertial GWs.

R: we have attempted to make this clearer where we describe the minimum required horizontal length scale (now taken to be 500 km).

3) Fig.2: it would be the best to add a panel showing how your vertical wavelength (Lz) change with decreasing the vertical resolution for, e.g., 5-day, 10-day, 15-day, and 20-day waves.

R: we agree and have added this panel to Fig. 2.

4) P13, L2: I strongly suggest you to elaborate the reason to explain the discrepancies among different datasets here more thoroughly, e.g., SABER retrieved temperature profiles or ERAi might have too coarse vertical resolution, etc. Then briefly summarize this point in the conclusion section.

R: since the background state for these values is easterlies, our resolution tests would suggest that larger vertical length scales should result in underestimation of the flux. We have added additional text about this wind state-resolution relationship in Section 3. Thus, while we acknowledge that coarse vertical resolution in these data will result in errors, it is not clear that Section 4 is the appropriate place to discuss this. Instead, we bring up the comparison to show that we are confident in our estimates. We have included additional text in the Summary giving further elaboration to these ideas, however.

5) P15, L16: I don't quite understand. KWMF plays a critical role in the descending of the QBO westerly phase, which shows a discernable enhancement along the zero-wind-line, as also shown

in Fig. 4 and Fig. 5. Then, when you do the composite, it seems to me that the KWMF enhancement actually occurs when the QBO easterly starts to weaken. Why?

R: in the previous versions of Figs. 4 and 5, there were too many missing points in the core of the easterlies to notice how large the fluxes were. This has been corrected for this new submission. You are correct that that the KWMF is critical in the transition, but the acceleration from the flux is strongest where (the negative of) the vertical gradient is largest. In Fig. 7, this occurs where along the regions of large vertical gradients in zonal wind. The text as written was not clear about this, so we have edited it.

6) P17, L28 and onward about the MJO discussion: firstly, you need to give a reference or two suggesting that MJO likely impacts the KWMF. As you later on stated that some of the previous studies also found that Kelvin waves were also released when MJO was in the inactive phase: then why conduct such an investigation?

If you'd like to study whether convective activities are tied to KWMF strength, simply use the daily OLR index for a given grid box around the sounding site, and set up a threshold to separate active and inactive convective days to composite the KWMF.

R: thank you for this suggestion. It seems obvious now that the first step in our presented analysis should have been to show the OLR-KWMF connection. We have determined a useful diagnostic of convective coverage upstream of the sounding site(s) that, once above a given threshold, allows us to find events for which the KWMF significantly rises above the background values. We then take these events and compare those with the strongest and those with the weakest MJO signal. From this, we believe we have found a meaningful signal in KWMF from the MJO. Perhaps key to this was ensuring that convection is active during the MJO events we analyze.

We believe that this is a sensible step in the knowledge of the field. If convection leads to stratospheric KWMF, then the MJO – the dominant pattern of intraseasonal variance in tropical convection – should have a discernable signal in stratospheric KWMF. While we strongly doubt that this idea is new to the field, there are not published studies about this to our knowledge. The work of Kiladis et al. (2005) does show penetration into the stratosphere of Kelvin wave-like perturbations during the MJO. This final bit of work was an attempt to begin connecting those dots. With the new means of analysis contained in the Discussion section, we hope that our attempts to make this tie are less abruptly introduced to the reader.

7) Like I said in the beginning, add some sentences or paragraphs highlight the uniqueness and novelty of your work.

R: we have added extra text in the introduction and summary noting that our long-term record of data and our application of short-time Fourier transforms are both novel. Our resolution experiments are novel as well, but drawing explicit attention to this seems inelegant where it would be in context.

Intraseasonal to interannual variability of Kelvin wave momentum fluxes as derived from high-resolution radiosonde data

Jeremiah P. Sjoberg[1,2], Thomas Birner[1], and Richard H. Johnson[1]

[1]Department of Atmospheric Science, Colorado State University, Fort Collins, CO 80521
[2]now at: COSMIC Project Office, University Corporation for Atmospheric Research, Boulder, Colorado

Correspondence to: Jeremiah P. Sjoberg (sjoberg@ucar.edu)

Abstract. Observational estimates of Kelvin wave momentum fluxes in the tropical lower stratosphere ~~remains~~ remain challenging. Here we extend a method based on linear wave theory to estimate daily time series of these momentum fluxes from high-resolution radiosonde data. ~~Testing the sensitivity to vertical resolution, our estimated momentum fluxes are found to be most sensitive to vertical resolution greater than 1 km, largely due to overestimation of the vertical wavelength. Estimates of momentum fluxes derived from reanalyses and coarse-resolution satellite data are notably larger.~~ Daily time series are produced for sounding sites operated by the U.S. Department of Energy (DOE) and from the recent Dynamics of the Madden-Julian Oscillation (DYNAMO) field campaign. Our momentum flux estimates are found to be robust to different data sources and processing, and in quantitative agreement with estimates from prior studies. Testing the sensitivity to vertical resolution, our estimated momentum fluxes are found to be most sensitive to vertical resolution greater than 1 km, largely due to overestimation of the vertical wavelength. Climatological analysis is performed over ~~the~~ a selected 11 year span of data from ~~the ARM~~DOE Atmospheric Radiation Measurement (ARM) radiosonde sites. Analyses ~~for the available~~ of this 11-year span of data reveal the expected seasonal cycle of momentum flux maxima in boreal winter and minima in boreal summer, and variability associated with the quasi-biennial oscillation ~~(QBO)~~ of maxima during easterly phase and minima during westerly phase. ~~Analysis of~~ Comparison between periods with active convection that is either strongly or weakly associated with the Madden-Julian Oscillation (MJO) ~~active periods~~ suggests that the MJO provides a nontrivial increase in the lowermost stratospheric momentum fluxes~~, though statistical significance is not found due to the small number of events observed in the available time series~~.

1 Introduction

Atmospheric equatorial Kelvin waves represent a tropical eastward propagating wave disturbance generated primarily by convection. As tropical convection is nearly ubiquitous, particularly near to the Intertropical Convergence Zone, Kelvin waves are regular phenomena. These equatorially trapped waves have zero meridional wind perturbations and are a consequence of the equatorial beta-effect (Gill, 1982). Convectively coupled Kelvin waves are important for tropospheric phenomena, such as the Madden-Julian Oscillation (MJO) and the El ~~Nino Southern~~ Niño-Southern Oscillation (ENSO) (Straub et al., 2006; Kiladis et al., 2009). These interactions arise from the eastward emanation of energy associated with these waves. Energy is

also emitted upwards by Kelvin waves into the tropical tropopause layer (TTL). In particular, these waves transport westerly momentum from the troposphere into the TTL and above.

Due to this upward flux of westerly momentum, Kelvin waves are known to influence the downward progression of stratospheric westerlies that occur during ~~a~~ the roughly 28 month cycle of winds known as the ~~Quasi-Biennial~~ quasi-biennial oscillation (QBO). There ~~is an established connection~~ are established connections between the QBO and midwinter polar stratospheric variability (Garfinkel et al., 2012), large-scale extratropical weather patterns (Thompson et al., 2002), and ~~ozone~~ stratospheric chemistry (Randel and Wu, 1996). Prior studies have shown that the QBO affects the vertical extent of convection (Collimore et al., 2003)~~and,~~ , and stratospheric water vapor through modulation of the cold-point temperature ~~, affects stratospheric water vapor~~ (Fueglistaler and Haynes, 2005).

Phasing of the QBO is initiated in the upper stratosphere by gravity waves of ~~identical~~ opposite propagation direction to that of the winds (e.g. for westerly winds, westward-propagating gravity waves drive reversal to easterlies; Baldwin et al., 2001). In the middle to lowermost stratosphere, additional waves come into play in each phase: Rossby waves and mixed Rossby-gravity waves during westerly phases and Kelvin waves during easterly phases. ~~The various wave modes propagate upwards until they reach a critical level (i.e. where the background wind matches the phase speed of a given wave) and dissipate, depositing the transported momentum. The oscillation of the QBO is a manifestation of this wave-mean flow interaction.~~ For a given state of the zonal winds (e.g. easterly), waves with phase ~~speed~~ velocity in the direction of the mean flow (e.g. Rossby waves) encounter a critical level in the lower stratosphere and are inhibited from propagating. Meanwhile, waves with phase speed in the opposite direction to the mean flow (e.g. Kelvin waves) are free to propagate through the stratosphere until they dissipate or encounter a critical level, depositing their momentum. After sufficient momentum deposition forces the background winds to reverse direction~~(e.g. from easterly to westerly)~~, the waves that forced the new wind state ~~(e.g. Kelvin waves)~~ are no longer able to propagate, allowing the other regime of waves ~~(e.g. Rossby waves) to propagate and force the zonal wind back to the initial direction (e. g. from westerly to easterly).~~ to continue the oscillation. See Baldwin et al. (2001) for a thorough review of QBO theory and impacts.

A missing component from our understanding of the interaction between Kelvin waves and the QBO is a precise measure of the actual vertical transport of ~~vertical~~ zonal momentum. This transport quantity is most typically written as the eddy ~~vertical~~ momentum flux $\rho\overline{u'w'}$, the density-weighted zonal mean of the product between zonal mean deviations of zonal wind u and vertical wind w. In principle, quantification of this flux only requires knowledge of the zonal distribution of these two fields. Measuring zonal wind does not present any considerable challenges as it has both ~~characteristic~~ typical speeds that are well above instrument sensitivity and large zonal coherence. Vertical wind, in contrast, does not display either of these ~~advantages: characteristic~~ characteristics: typical vertical wind speeds are on the order of 1 cm s^{-1} and zonal variations are large. While some observational platforms – such as flux towers – may reasonably estimate the vertical winds, they are spatially inhomogeneously distributed and only measure within the boundary layer.

Observational shortcomings such as these do not prevent estimation of the Kelvin wave momentum fluxes, however. Maruyama (1968), through judicious application of dynamical theory, showed that the covariance of zonal wind and vertical wind may be approximated by the quadrature spectrum of zonal wind and temperature. That is, the out-of-phase relationship between these

two readily observable fields ~~– zonal wind and temperature –~~ may be used to estimate the vertical momentum fluxes by Kelvin waves. Later studies based on radiosonde data showed that these waves account for a non-negligible portion of the westerly momentum when the QBO is in its easterly phase (e.g. Sato et al., 1994; Maruyama, 1994). Other theory-based estimates of momentum fluxes have been derived for use with satellite irradiances (Hitchman and Leovy, 1988; Ern and Preusse, 2009) and have found similar magnitudes of the momentum fluxes. Together with estimations using reanalysis products (e.g. Tindall et al., 2006), qualitatively consistent bounds to the momentum flux amplitudes have been determined.

Yet there remain places where our understanding and estimation may be improved. For instance, few climatological analyses of Kelvin wave momentum fluxes have been performed. While satellite and reanalysis studies have long data records over which to analyze, the vertical resolution of both data sources is greater than a kilometer in the lower stratosphere. It is not clear how sensitive momentum flux calculations are to vertical resolution, particularly for lower stratospheric Kelvin waves with vertical wavelengths on the order of 2-4 km. Kim and Chun (2015) ~~show~~ showed that such waves may be significantly under-resolved in reanalyses. Studies using high vertical resolution radiosonde data meanwhile only analyzed broad characteristics of Kelvin waves during easterly and westerly QBO phases (e.g. Sato and Dunkerton, 1997), or point estimations of the flux amplitudes (e.g. Holton et al., 2001).

Here we extend previous methods using radiosonde data to analyze climatologies, variabilities, and vertical resolution ~~dependence~~ dependences of Kelvin wave momentum fluxes. We make use of both quality-controlled, high resolution data from a recent field campaign and raw, high resolution data from long-term radiosonde stations. We apply an algorithm for producing continuous, daily time series of momentum flux estimates. By varying the vertical stepping of input data to the algorithm, we determine the role of vertical resolution on estimations of the fluxes. ~~We then analyze the annual cycle and QBO cycle~~ Because we utilize a relatively long-term dataset, we are able to analyze the intraseasonal and interannual variability of these time series of momentum fluxes, demonstrating that our methodology reproduces expected qualitative structures. From our estimates of the flux, we find evidence that a positive contribution to the momentum flux variability is provided by convection associated with the MJO.

Section 2 describes the data and methods we use to generate our flux estimates. Vertical resolution dependence is discussed in Section 3. We present time series of our results in Section 4. ~~Two~~ The annual mean and QBO-mean climatologies are discussed in Section 5. We ~~finish by summarizing and discussing our findings~~ discuss implications of these results in Section 6 and summarize in Section 7.

2 Data and methods

2.1 Data

~~We primarily use radiosonde data~~ The radiosonde data we use come from two sources. The first source contains short-term but high resolution data from the Dynamics of the Madden-Julian Oscillation (DYNAMO) field campaign (Yoneyama et al., 2013). One objective of DYNAMO was to analyze initiation of the ~~Madden-Julian Oscillation (MJO)~~MJO, in part through collection of frequent high-resolution radiosonde data. We use Level 4 radiosonde data (see Ciesielski et al., 2014) from the Gan Island

(0.7°S, 73.2°E) and Manus Island (2.0°S, 147.4°E) sounding sites. These Level 4 data are produced at 50 m vertical resolution and 3-hourly temporal resolution. The Gan Island data span from 22 September 2011 to 08 February 2012, while the Manus Island data span from 24 September 2011 to 30 March 2012.

The second radiosonde source contains lower temporal resolution but longer spanning data from two U.S. Department of Energy Atmospheric Radiation Measurment (ARM) program sounding sites: Manus Island and Nauru Island (0.5°S, 166.9°E). See Mather and Voyles (2013) for a review of ARM facility instruments and missions. Data are recorded every 2 seconds, corresponding to a vertical step of roughly 10 m, by the sounding packages on launches with frequency ranging from once daily ~~early in the data record~~ to 8 times daily during intensive operation periods such as DYNAMO. The number of data early within the record are insufficient for the spectral filtering we apply so we only consider data from 2003 January 01 to 2013 December 31 for this study. Sondes were launched at least twice daily during this 11 year range.

Data from the European Centre for Medium Range Weather Forecasting (ECMWF) Interim Reanalysis (ERAi) are also used (Dee et al., 2011) for estimating momentum fluxes and for zonal mean zonal winds. The data are on a regular 0.75° grid in longitude and latitude, and are given at six-hourly temporal resolution. Model level data are used here to take advantage of the highest available vertical resolution in the TTL (∼1000-1500 m).

~~For composites about the Madden-Julian Oscillation (MJO) , we use both the Real-time Multivariate MJO (RMM) index (Wheeler and Hendon, 2004) and the OLR-based MJO~~Outgoing longwave radiation (OLR) data are from a long-term record of daily, 1° x 1° gridded observations retrieved primarily by the high-resolution infrared radiation sounder instruments on board the National Oceanic and Atmospheric Administration (NOAA) TIROS-N series and Eumetsat MetOp polar orbiting satellites. These data, developed by a joint partnership between NOAA and the University of Maryland are obtained from the NOAA National Centers for Environmental Information (https://www.ncdc.noaa.gov/news/new-outgoing-longwave-radiation-climate-data-record

For analyzing the MJO, we use the OLR MJO Index (OMI) index (Kiladis et al., 2014). ~~Both indices are~~ OMI is based on the principal component time series of the first two ~~empirical~~ empirical orthogonal functions of ~~their input atmospheric fields. For the RMM index, these atmospheric fields are outgoing longwave radiation (OLR) and zonal winds at both 850 hPa and 200 hPa. For the OMI , the only atmospheric field is OLR. As we are most interested here in the generation of Kelvin wave momentum fluxes by convection, we only show MJO composite results using OMI. MJO composites using the RMM index are not qualitatively different~~20°S-20°N, 20-96 day filtered OLR. OMI data are obtained from the Physical Sciences Division of the NOAA Earth System Research Laboratory (https://www.esrl.noaa.gov/psd/mjo/mjoindex/).

2.2 Methods

To ~~standardize the vertical and temporal resolutions of the data we use~~grid the radiosonde data, raw data are linearly interpolated in height and cubic spline interpolated in time. To constrain the interpolation, we require that each output data point ~~have~~ has at least 3 input data points within the span from 3 days prior to 3 days following, and at least 3 input data points within the span from 500 m above to 500 m below. Note that this interpolation does not fill all gaps, allowing for missing data to remain. The results are not significantly different for other ~~combinations of linear and spline~~ orders of interpolation, nor for changes ~~to~~ in

the time range or spatial range in which data points must exist in order to interpolate to a specified output point. ~~An exception to this is~~ This does not hold if the time range or spatial range is too small ~~(~~ – shorter than 1 day or less than 100 m, respectively ~~)~~ – in ~~this~~ which case few output points will be produced.

We range the output temporal resolution ~~Δt_{win}~~ from 6 hours to 48 hours, and the output vertical resolution ~~Δz_{win} from 50~~ from 100 m to 2000 m. These ranges are used to study resolution effects on the calculated momentum fluxes. For our standard analysis, we ~~show~~ use temporal resolution of 24 hours and vertical resolution of 250 m. ~~Motivation for~~ While daily data are standard for the field, motivation for why we use ~~these values~~ vertical stepping of 250 m is given in the next section.

To estimate the Kelvin wave momentum fluxes, we follow the technique described in Sato and Dunkerton (1997) and Holton et al. (2001). Wave solutions to the linearized equatorial beta-plane equations result in

$$\rho\overline{u'w'} = -\rho\frac{R\omega_d}{HN^2}Q_{uT}\,, \tag{1}$$

where R is the gas constant; H is the scale height of the atmosphere, taken to be 7 km here[1]; N^2 is the squared Brunt-Väisälä frequency; Q_{uT} is the quadrature spectrum between u and temperature T, given in units of K m s^{-1}; and ω_d is the intrinsic frequency. Inclusion of density ρ in Eq. (1) casts the momentum flux as a stress term (in units of mPa) ~~from~~ of which the vertical gradient approximates the Transformed Eulerian Mean wind forcing

$$\partial_t\overline{u} \propto -\rho^{-1}\partial_z\left(\rho\overline{u'w'}\right)\,. \tag{2}$$

Following Andrews et al. (1987), with no meridional wind perturbations v' and the ~~WKB~~ WKBJ assumption, the intrinsic frequency takes the form

$$\omega_d \equiv \omega - k\overline{u} = -\frac{kN}{m}\,. \tag{3}$$

Here, k is the zonal wavenumber satisfying $k = 2\pi/L_x$, where L_x is the zonal wavelength of the Kelvin waves. m is the vertical wavenumber and is defined to be negative. In deriving the intrinsic frequency, we assume that both the zonal mean zonal wind and stratification N^2 vary in the vertical and in time, but that variations ~~in the stratification are small relative to the vertical wavelength~~ are slow relative to variations in the phase of the waves~~L_z. This latter~~. While this condition is generally true in time and space, variations in zonal wind can be large such that our estimates of the flux near, say, regions of QBO wind transition are more uncertain. WKBJ approximations, and thus the applied wave solutions used in deriving Eq. (1), may not be applicable in these regions. But as shown later in Section 4, we find good agreement between our results and those from previous studies, lending credibility to our estimates.

For stratification, this slowly-varying assumption is true above the tropopause inversion layer (TIL, e.g. Grise et al., 2010), and we find that 18 km typically lies above the TIL. We thus set the lower boundary of our ~~analysis~~ analyses to this level. For the upper boundary of our analyses, 30 km is a natural choice as few radiosondes reach or extend beyond this level. To highlight results in the lowermost statosphere, we use 25 km as an upper boundary for the presented figures.

[1]Although this scale height is too ~~short~~ long for the lower stratosphere, it is the value used in the literature (e.g. Andrews et al., 1987). Hence, we use 7 km to be consistent with past studies.

The values of ω, i.e. the frequencies relative to the ground, are determined by the frequency bands of the spectral transform we apply to the sounding data. These bands are determined by the time stepping of our data and by the windowing of our spectral decomposition – here taken to be 40 days. This window length allows us to calculate the momentum fluxes at the principal Kelvin wave periods that lie between 5 and 20 days. For the 40 day windowing, the central periods are 20, 13.3, 10, 8, 6.7, 5.7 and 5 days.

The zonal means of both zonal wind and temperature are approximated by their time mean over each window. Such an approximation is reasonable in the stratosphere. We have compared our estimates of the zonal mean fields to those calculated from ERAi and found that the fields do not qualitatively differ. From our approximations of $\overline{u}$ and $\overline{T}$, we calculate the zonal deviation fields u' and T', and the stratification N^2.

Vertical wavenumbers m are estimated by modifying a method described in Holton et al. (2001). For each data window, we filter u' and T' for each frequency band using a Butterworth bandpass filter. Then for each of the 40 days within each data window, we find the longest vertically contiguous span of data between 15 and 30 km for both fields at all temporal frequencies. 15 km is used as it represents the upper boundary of convection (e.g., Feng et al., 2014; Xu and Rutledge, 2015) from which Kelvin waves will emanate. The vertical quadrature spectrum $Q_{uT,v}$ is calculated from these contiguous spans of data. From the vertical wavelengths that have phasing such that temperature leads zonal wind, we select the wavelength with the largest negative value of $Q_{uT,v}$. ~~This results~~ The phase difference between temperature and zonal wind is required to be 45°-135° so as to avoid ambiguity for phase differences close to 0° and 180°. These steps result in an estimate of L_z for each of the 40 days in a given data window and for each temporal frequency band. We use the window-mean L_z to then calculate the vertical wavenumber ~~$m = 2\pi/L_z$~~ $m = -2\pi/L_z$.

This method of estimating the vertical wavenumber was applied to the Nauru99 data that Holton et al. (2001) analyzed. Their estimate of 4.5 km for wave periods of 9-11 days is ~~nearly the same as~~ close to ours of 4.0 km for the same wave periods. Likewise, our estimated range of 3.2-5.1 km vertical wavelength for wave periods of 4-6 days is very similar to the range of 3-4.5 km ~~estimate~~ by Holton et al. (2001).

~~By finding~~ With m ~~, we have all terms in~~ known, we may reorder Eq. (3) ~~except the~~ to obtain the relation for zonal wavenumber k~~, which can be obtained from the dispersion relation~~:

$$k = 2\pi/L_x = \omega/\left(\overline{u} - \frac{N}{m}\right). \tag{4}$$

~~To ensure that we analyze~~ For positive ω and sufficiently strong easterlies, Eq. (4) results in negative k. Since k is defined to be positive for Kelvin waves, ~~we impose contraints on where the estimated k~~ such regions – ~~and thus momentum flux~~ most often found in strong easterlies critical to QBO evolution – ~~are valid. We require that the intrinsic zonal phase speed $\omega_d/k > 0$. We further constrain our analyses to wavelengths greater than 100 km, which captures the observed dominant horizontal Kelvin wave scales of ~1000 km or larger. Taken together, these constraints require that $k > 0$.~~

~~The requirement of positive zonal wavenumber impacts our calculated momentum fluxes because,~~ must be excluded from our analysis. But, there is no sign constraint imposed on ω. We make use of this and of the symmetry of spectral amplitudes about positive and negative ω, i.e. the spectral amplitude $\hat{\chi}$ for a given field χ has the following characteristic: $\hat{\chi}(\omega) = \hat{\chi}(-\omega)$.

Since we know the spectral amplitudes for positive ω, we simply select the sign of ω such that k is positive from Eq. (4), ~~regions of strong easterlies (e. g. where $\overline{u} < -20$ m s^{-1}) often result in negative k. Because our method assumes that there is a constant vertical wavenumber for a given window of data, it is not able to properly estimate the changes in zonal wavenumber with height, particularly where the zonal wind varies a lot~~. This however allows the estimated values of L_x to be small ($\ll 100$ km) where we flip the sign of ω. Since short zonal wavelength Kelvin waves are indistinguishable from gravity waves (**?**), we constrain our calculations to points where the horizontal wavelengths are greater than 500 km. We also require that the intrinsic zonal phase speed ω_d/k be positive, a fundamental requirement for Kelvin waves.

Anywhere the above constraints are violated, we set the momentum fluxes to be missing. In order to restrict the impact of these eliminated regions on the analysis presented below, we only retain those points for which every frequency band has real data. This is perhaps more restrictive than is necessary, but ensures consistency, particularly for climatological analyses.

An additional constraint we could apply is that the meridional wind perturbations v' be negligible. This is an important distinguishing property between Kelvin waves and inertio-gravity waves. Appropriately implementing this constraint here is imprecise, however. Unlike with zonal wind, the assumption that the time mean approximates the zonal mean of meridional wind is not accurate. Our estimates of v' will not then be representative of wave perturbations from the zonal mean. Nevertheless, we have tested only retaining data points that fulfill $|v'| < 5$ m s^{-1} and found that our results are not significantly altered by that. Hence, we refrain from applying this constraint.

With all inputs known for Eq. (1), we calculate the momentum flux for each temporal frequency band between 5 and 20 days. Our method of calculation is performed at consecutive windows spaced ~~Δt_{win}~~ 1 day apart. We then concatenate all these data windows to produce a daily time series of total Kelvin wave momentum fluxes. For this time series, the dates of the momentum fluxes ~~we calculate is~~ are set to the middle date of each window. This technique of calculating spectral amplitudes in overlapping windows is more commonly referred to as a short-time Fourier transform (STFT). The use of STFT differs from prior work which used non-overlapping windows of data to estimate momentum flux. As a result, we have an effecitvely higher temporal resolution, allowing for greater detail in analyses of intraseasonal and interannual variability of the estimated flux.

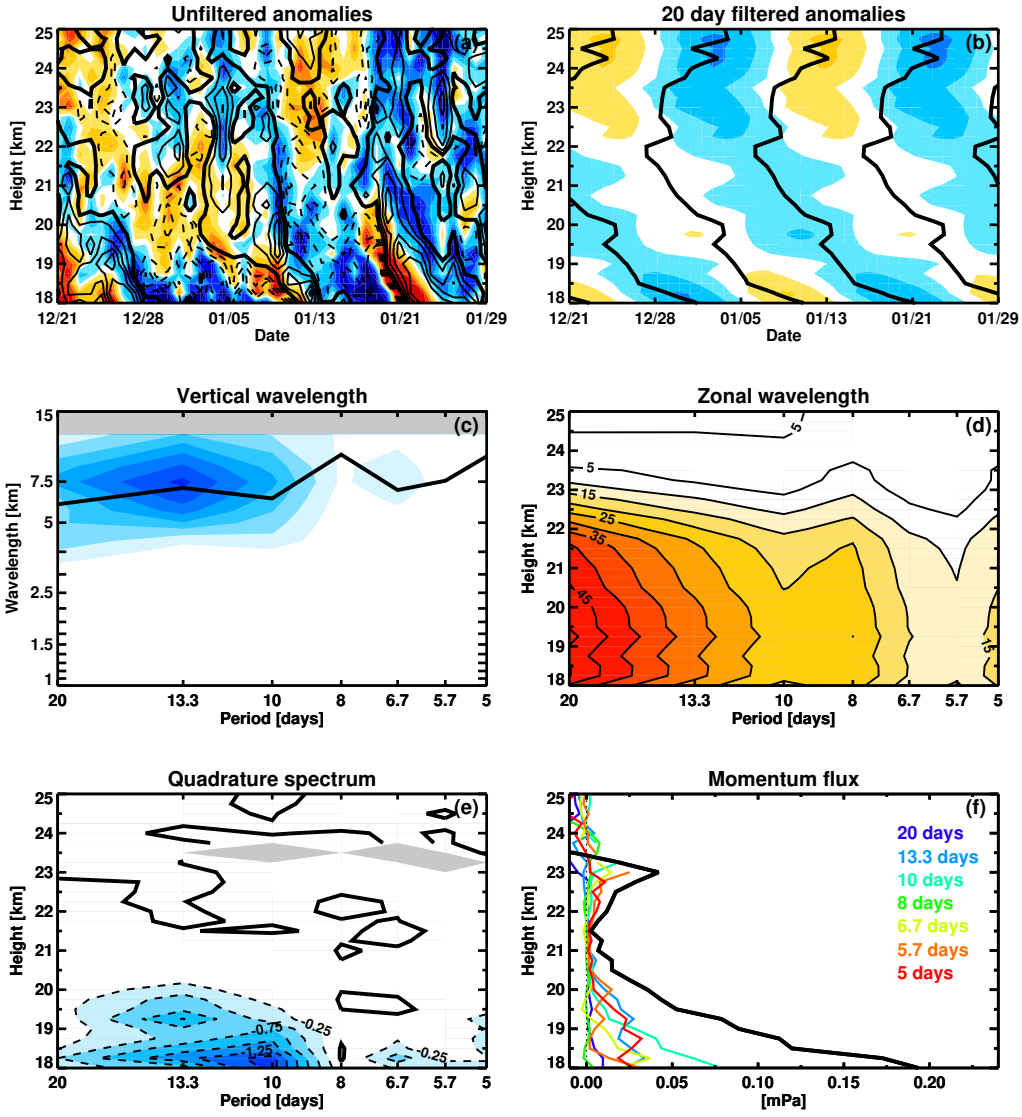

Figure 1. An example of the Kelvin wave momentum flux calculation for Gan Island over the 40 day window between 21 December 2011 and 29 January 2012. (a) Unfiltered zonal temperature anomalies (shading) and zonal wind anomalies (contours). The zonal wind and temperature contour intervals are 3 m s^{-1} and 1 K, respectively. (b) 16-27 day bandpass filtered temperature and zonal wind over the data window. These correspond to the 20 day period waves in our calculations. (c) ~~Vertical~~ 40-day mean vertical quadrature spectrum between u′ and T′ (shading) as a function of period and vertical wavelength, and calculated vertical wavelength (black curve, units km) as ~~functions~~ a function of ~~filtering window~~period. Dark blue shading indicates large magnitudes of the quadrature spectrum. (d) Zonal wavelength as a function of height and of ~~filtering window~~period. Units are 1000 km. (e) The temporal quadrature spectrum between u′ and T′. Units are K m s^{-1}. (f) The calculated total 5-20 day momentum flux (black curve) as a function of height. The colored curves show the contributions from individual ~~filtering windows~~periods.

2.3 Example

An example of our method of calculation is shown in Fig. 1. The data for this example are from Gan Island and cover the 40 day window between 21 December 2011 and 29 January 2012. Unfiltered temperature anomalies (shading) and zonal wind anomalies (contours) are shown in panel (a). The estimated zonal mean zonal wind for this data window may be seen in the top panel of Fig. 3. The signature of Kelvin waves is present here: temperature anomalies lead zonal wind anomalies of the same sign with a roughly 90° phase difference. To better highlight this, panel (b) shows 16-27 day (20 day central period) bandpass filtered temperature and zonal wind. From these filtered anomalies, we expect to find large Kelvin wave momentum fluxes in the region between 18 and 21 km.

Panel (c) shows ~~in shading~~ the mean vertical quadrature spectrum as a function of vertical wavelength and frequency in shading. The associated estimate of the vertical wavelengths is overplotted by the black curve. For this window, the waves we analyze have vertical wavelengths between 5-10 km, which fall well within ~~typical~~ observed ranges of vertical wavelengths ~~of~~ for equatorial Kelvin waves (e.g., Randel and Wu, 2005).

Zonal wavelengths are shown in (d) as a function of height and of wave period. The longest waves are at the longest periods and primarily below 21 km~~, as expected from visual inspection of (a). Above ~23.5 km, the wavelengths are negative for all periods other than 5 days. Since negative L_x is not consistent with the theory used here, we exclude any such regions (gray shading).~~ .

Panel (e) shows the quadrature spectrum between zonal wind anomalies and temperature anomalies as a function of period and of height. These spectra are used for calculation of the momentum fluxes shown in panel (f). As expected, the total momentum flux is large between 18 and 20.5 km with a roughly linear decrease in magnitude throughout this vertical span. Above this, the momentum flux is nearly constant with only ~~slight~~ moderate variations up to 25 km. The calculated fluxes in (f) are assigned to 09 January 2012, the central date of the window. Note that the wavenumbers and frequencies derived from the results shown in Fig. 1 are consistent with Kelvin waves (cf. Fig. 3 of Wheeler and Kiladis, 1999).

3 Resolution dependence

We test the dependence of the calculated momentum flux amplitudes on the resolution of input data by independently varying the vertical and temporal resolutions of the imposed interpolation. These tests are performed for a reference level of 18 km. We carry out the following tests at levels above 18 km and find that the results qualitatively hold. At higher levels, a number of complicating effects may come into play. First, coexistence of strong easterlies and relatively short vertical wavelengths ~~occur~~ occurs frequently above 20 km. As ~~discussed in the previous section~~these two conditions tend to result in horizontal wavelengths shorter than 500 km, such regions violate the assumptions that allow the derivation and application of Eqs. (1) and (3). Second, with increasing height, data gaps ~~are increasingly likely~~ increase as balloon bursts limit the maximum height of radiosondes. By analyzing just above the tropopause, we are more likely to minimize the impacts from these complications.

~~To consistently compare the effects of changing vertical and temporal resolutions, we first take the time mean of each of the input fields to Eqs. (1) and (3). Doing so underestimates the true time mean of the momentum fluxes by an average error of~~

~~~3%, but allows us to test which inputs most strongly change the calculated fluxes as either the vertical or temporal resolution is changed. We also only use those data points that are not missing in any of the tested resolutions (total of 377 points).~~

Fig. 2 (a) shows, as a function of vertical resolution, the mean 5-20 day Kelvin wave momentum fluxes over these common points (solid black). Values of the momentum flux are given on the right axis while percent differences from the reference calculation using 250 m vertical resolution are given on the left axis. The percent difference is defined here as $PD = (M - M_0)/((M + M0)/2)$ where M is the value at each vertical resolution, and M_0 is the reference value. For this analysis, we only use those data points that are not missing in any of the tested resolutions (total of 3240 points).

There is a strong linear relationship between the vertical resolution and the percent differences of the calculated momentum fluxes, with a mean increase of ~~1.4~~$\sim$1.2% ~~difference~~ for every 100 m increase in vertical stepping. The standard errors of each measurement are shown with error bars for each tested resolution, where the number of input points has been reduced by the e-folding time scale of the momentum flux data (23 days). The difference between the mean flux at 250 m and those at both 1800 m and 2000 m are significantly different at the 90% level.
~~~

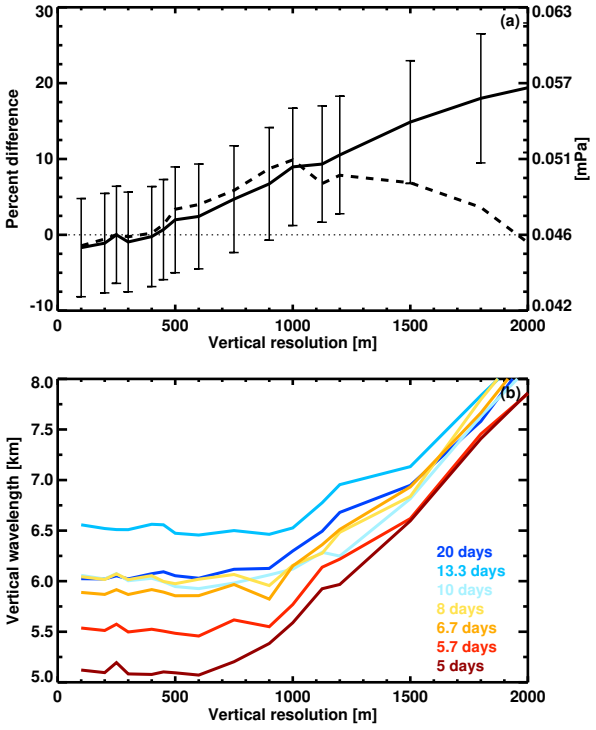

Figure 2. (a) Percent difference in ~~time mean~~ the momentum fluxes from 250 m vertical resolution (solid). The right axis gives the values of the ~~mean~~flux. The dashed curve shows values for calculations done with L_z set to the 250 m resolution values. Standard errors are shown with bars for each tested resolution. (b) ~~Percent difference from 24 hour temporal resolution (solid).~~ The ~~dash-dot curve shows values for calculations done with Q_{uT} set to the 250 m~~ variation of vertical length scale as a function of vertical resolution~~values~~, shown here for each analyzed wave period.

We also study the impact of holding individual input parameters constant at the 250 m resolution ~~value and repeated the calculation~~values. The inputs considered here are stratification N^2, horizontal length scale L_x, vertical length scale L_z, and quadrature spectrum Q_{uT}. Holding N^2, L_x, or Q_{uT} steady is found to not strongly influence the calculated fluxes: the momentum fluxes still increase for increasing vertical resolution at roughly the same rate (not shown).

In contrast, for constant vertical wavelength (dashed), the calculated fluxes increase to 900 m resolution and then decrease for still larger vertical stepping. This suggests that a large portion of the dependence of momentum fluxes on vertical resolution greater than 1000 m results from changes in the vertical wavelength. ~~To demonstrate how strong this dependence is, the dashed curve shows the mean fluxes if all inputs except~~ Panel (b) shows the how the vertical wavelength ~~are held constant at the 250 m value~~varies as a function of vertical resolution. Up to ~~900~~ ~1000 m resolution, ~~there is little dependence on~~ the vertical wavelength is insensitive to vertical resolution. ~~Beyond, the fluxes increase rapidly, reaching the same values at 2000 m as those for which all inputs are allowed to vary~~From 1000 m to 2000 m resolution, the mean vertical wavelength at all

wave periods linearly increases to be greater than 7.5 km. Notably, the minimum vertical wavelengths (not shown) have an analogous dependence: below 1000 m vertical stepping, the wavelength minima are all approximately 2 km, whereas these minima necessarily increase to be greater than 5 km by 2000 m stepping.

~~Fig.~~ Performing analytic experiments with Eqs. (1)-(4) verify that overestimation of the vertical wavelengths leads to overestimation of the momentum flux if the background wind is westerly. In easterlies, the effect is reversed but of relatively smaller magnitude, i.e., a given overestimation of vertical wavelength in westerlies increases the flux more than it is decreased in easterlies. Note that this relationship implies that the mean zonal wind for the points analyzed in Fig. ~~2 (b)shows the results from a similar analysis performed for changing temporal resolution. For changes in time stepping, the quadrature spectrum Q_{uT} has the strongest influence on the calculated momentum fluxes. By holding it steady at the 24 hour value (dash-dot), the fluxes remain nearly steady across a range of time resolutions.The primary result here, however, is that the overall variations in calculated momentum fluxes~~ 2 are westerly (see Fig. 6).

A similar analysis for changing temporal resolution finds that the overall variations from changes in ~~temporal resolution~~ time stepping are much smaller than those from ~~changes in vertical resolution .~~ vertical resolution (not shown). For time steps between 0.25 to 2 days, the mean flux is at most 5% different from the value for 24 hour resolution.

4 Time series results

Fig. 3 shows time series of 5-20 day Kelvin wave momentum fluxes calculated from DYNAMO data collected at Gan Island (top) and Manus Island (bottom). Both time series capture the same qualitative structure: ~~enhanced~~ positive fluxes in October and November 2011, followed by a large, sustained burst of positive flux that begins in early January 2012. The vertical extents of these momentum fluxes in both time series are also comparable, with amplitudes in both cases negligible above $\sim$21 km. This agreement is verified through linear correlation coefficients between the two time series that are between 0.67 and 0.91 at all levels from 18 through 20 km. Lagged correlations do not suggest that there is a time offset between the two time series.

A noteworthy difference between the two is that the amplitudes at Gan Island are roughly 2-3 times larger than those at Manus Island. While this is certainly the case for the month of January, it is perhaps more obvious for the period between mid-October and mid-November. This amplitude difference arises in part because our method estimates the ~~full zonal mean~~ momentum fluxes from a point source of data. While Gan Island is located in a region of the Indian Ocean that is relatively far removed from other land surfaces, Manus island is located just to the east of the Maritime Continent. The Maritime Continent is known to diminish both Kelvin waves (Flannaghan and Fueglistaler, 2012) and convective signals ~~,~~ such as the MJO (Zhang, 2005) ~~,~~ that force these waves.

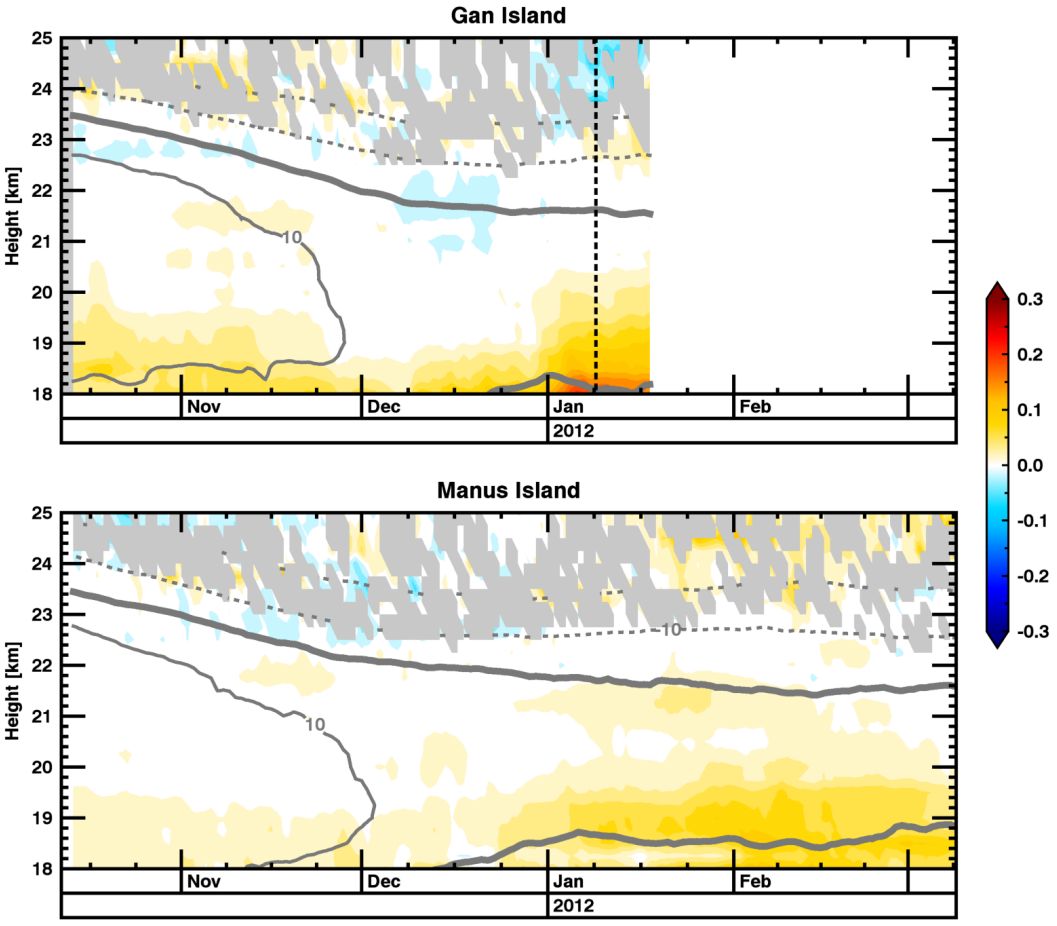

Figure 3. Time series of 5-20 day Kelvin wave momentum fluxes (shading) for Gan Island (top) and Manus Island (bottom) over the DYNAMO field campaign. The dark gray contours give the estimated zonal mean zonal wind at each site; solid contours are westerlies while dashed contours are easterlies. The 0 m s^{-1} contour is shown in bold gray. The vertical black dashed line denotes the central date of the window used in Fig. 1. ~~Gray~~ Light gray shading indicates where the momentum flux is not being calculated for any frequency band. Momentum flux is in units of mPa and zonal wind contour spacing is 10 m s^{-1}.

Figs. 4 and 5 show the time series of momentum fluxes for the Manus ARM site. We find that there is strong qualitative and quantiative agreement between momentum fluxes calculated from both the Manus and ~~Naura~~ Nauru ARM sites. See supplementary Figs. S1 and S2 for the time series of momentum fluxes from the Nauru ARM site.

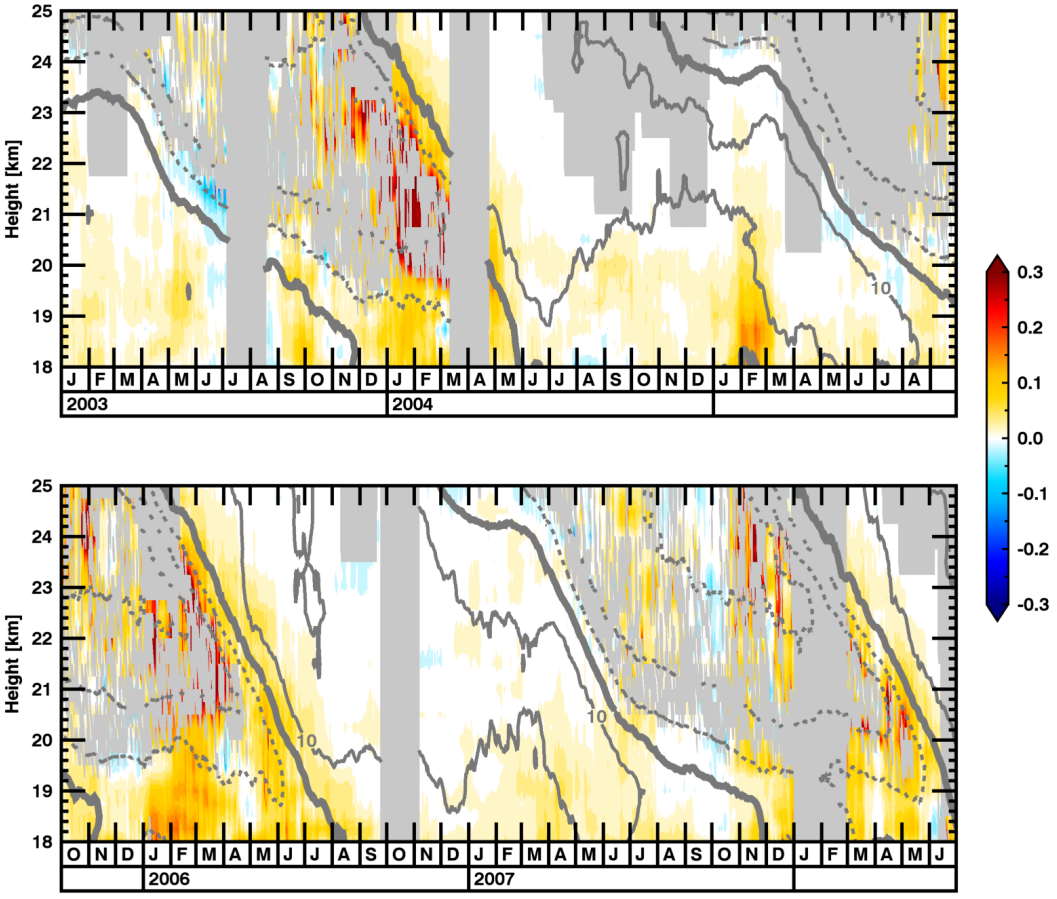

Figure 4. Time series of momentum fluxes from the Manus ARM site. Plotted fields are as in Fig. 3. The span here covers 01 January 2003 through 30 June 2008. Momentum flux is in units of mPa and zonal wind contour spacing (gray contours) is 10 m s^{-1}.

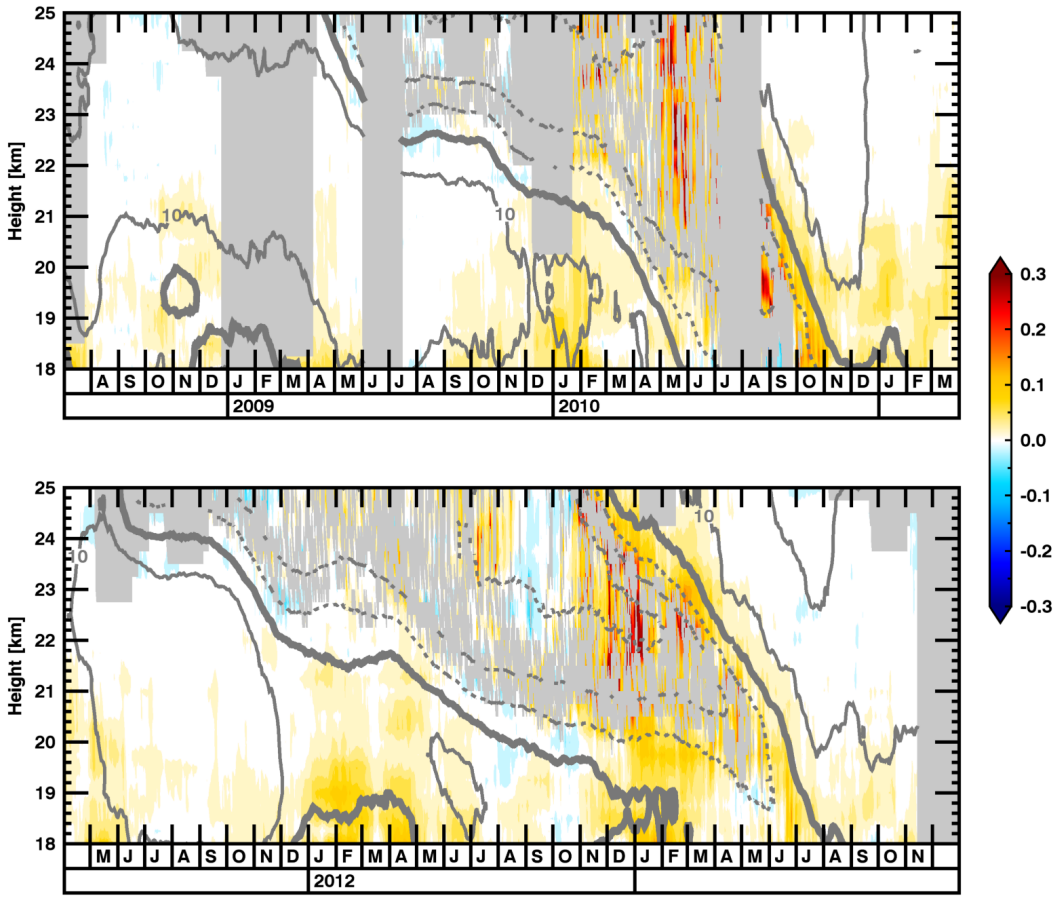

Figure 5. Time series of momentum fluxes from the Manus ARM site, continued. The span here covers 01 July 2008 through 31 December 2013.

In the time series, there are broad regions of data in the center of the easterlies in which the theoretical assumptions are violated (gray shading, see discussion in Section 2); these regions are excluded. ~~Outside of the exclusions~~There are also spans and heights with missing radiosonde data that are identifiable by the rectangular regions of gray shading. Where the data are not missing in easterlies, the qualitative patterns of the fluxes match expectations: Kelvin waves are influencing the descent of the westerlies by fluxing westerly momentum there. This is most clearly seen through descending maxima of the flux amplitudes that track the 0 m s^{-1} contour. In westerly QBO phases, these fluxes are nonzero but much smaller.

We find that our estimated momentum flux amplitudes qualitatively agree with those estimated by Ern and Preusse (2009, their Figs. 4 and 5), though with somewhat smaller amplitudes. For example, the momentum flux increase between 18-20 km for JFM in 2006 (bottom panel of Fig. 4) is identified in Ern and Preusse (2009), but their amplitude reaches at least 0.3 mPa

while ours is at most ~~0.25~~ ~0.20 mPa. A similar comparison with momentum fluxes derived from ERAi (not shown) also finds qualitative agreement with our amplitudes being smaller.

Calculated momentum fluxes for the Manus ARM site are remarkably similar to those from the Manus DYNAMO data, when the resolution between the two datasets is the same (cf. Fig. 3 and the lower panel of Fig. 5). The linear fit of these two datasets has a correlation coefficient of 0.94 and an offset less than 0.0006 mPa. Fidelity between momentum fluxes from both data sources is ~~advantageous to us~~encouraging, as the long record length of the ARM data greatly increases the time over which we can analyze the waves.

One interpretation of the above results that arises when comparing simultaneous calculations of momentum fluxes at different sounding sites (see Figs. 3 and 5) is as follows: our technique for calculating momentum fluxes is strongly influenced by the local conditions. For the DYNAMO data, Gan Island observations occur within the Indian Ocean where strong convection associated with the Madden-Julian Oscillation (MJO) is common. The expansive convection associated with these MJO events experienced at Gan Island propagates eastward to Manus Island, but is diminished after propagating over the Maritime Continent (Zhang, 2005). One would expect that such a disruption to the convection will lead to a disruption in the generation of Kelvin waves. This may, in part, explain why the estimated momentum flux amplitudes are smaller at Manus Island, located to the east of the Maritime Continent. Fluxes at Nauru, ~20° to the east of Manus, are similarly smaller (see Figs. S1 and S2).

Our calculated momentum fluxes largely represent local contributions to the zonal mean. However, stratospheric Kelvin waves are known to strongly project onto plantery scales (i.e. zonal wavenumbers 1-3, Feng et al., 2007). This projection may be in part from a quasi-stationary source of these waves: frequent convection over the Indian Ocean and Maritime Continent. It is possible that data from Indian Ocean sounding sites routinely sample the amplitude maxima of these planetary-scale wave momentum fluxes. Our results may then give an upper estimate of the flux amplitudes. Future, more detailed analyses may reveal more insight into this issue.

5 ~~Annual cycle and QBO~~

~~Manus Islandclimatological~~

5 Annual cycle and the QBO

The annual cycle of momentum fluxes and of input fields to the calculation of Eq. (1) for Manus Island are shown in Fig. 6. These ~~climatologies~~ mean fields are smoothed with a 21-day boxcar window for ease of viewing. In this and all remaining analyses involving averaging or compositing, we omit any points that have missing data. Note that this results in undersampling of the easterly winds in, e.g., Fig. 6 (a) since there are many missing data in this phase of the QBO (see Figs. 4 and 5).

Panel (a) shows that the lower stratospheric momentum fluxes maximize in January through March (JFM) and minimize in July through September. Each of the input fields to Eq. ~~1~~ (1) shows variations that reinforce the variations in momentum flux (panels b-d). Particularly in JFM, the zonal wavelengths become shorter, and the quadrature spectrum amplitude maximizes.

Panel (a) additionally shows that, over our data record, ~~the westerly QBO phase persists longer in the lower stratosphere than the easterly QBO phase. The momentum fluxes meanwhile are maximized (minimized) in winds that are more easterly (westerly), as expected. This QBO influence on momentum fluxes may more obviously be seen in Fig. 4 through the downward descending amplitudes that fill the region below the 0 m s^{-1} wind contour. Here we~~ despite the westerly phase persisting longer (see Figs. 4 and 5), the easterly phase of the QBO has stronger zonal winds above 21 km than those during the westerly phase.

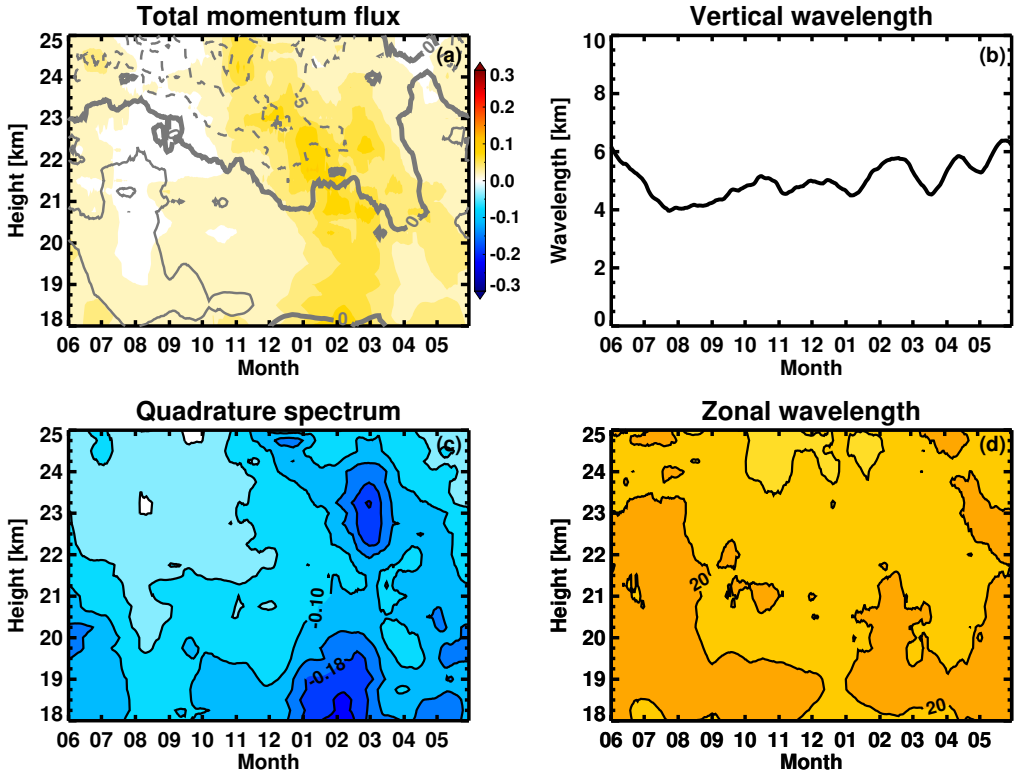

Figure 6. Climatology of momentum flux and related fields from the Manus ARM sounding site. (a) The 5-20 day total momentum flux [mPa] in shading and zonal mean zonal wind in contours. (b) The vertical length scale L_z [km]. (c) The quadrature spectrum Q_{uT} [K m s^{-1}]. (d) The horizontal length scale L_x [1000 km] with contour spacing of 5000 km. The vertical wavelength, quadrature spectrum, and zonal wavelength are means over all wave periods and all fields are smoothed with a 21-day boxcar filter.

We next analyze the typical momentum fluxes associated with the QBO.

~~Climatology of momentum flux and related fields from the Manus ARM sounding site. (a) The 5-20 day total momentum flux mPain shading and zonal mean zonal wind in contours. Note that the momentum flux scale is three-tenths of that in Figs. 3 and 4. (b) The vertical length scale L_z km. (c) The quadrature spectrum Q_{uT} K m s^{-1}. (d) The horizontal length scale L_x~~

Table 1. Average residence time and standard errors, in units of days, for each bin of QBO_i. Only the four full cycles of the QBO in our data are analyzed here.

Bin center	Residence time
-0.875	163 ±29.2
-0.625	40.3 ±5.15
-0.375	55.4 ±3.62
-0.125	35.0 ±4.56
0.125	175 ±56.3
0.375	99.5 ±35.2
0.625	83.8 ±27.1
0.875	168 ±54.9

~~1000 km. The vertical wavelength, quadrature spectrum, and zonal wavelength are period-weighted means and all fields are 21-day boxcar smoothed.~~

We determine phases of the QBO based on an index of the phasing between zonal mean zonal wind at 30 hPa (U_{30}) and at 50 hPa (U_{50}). Note that our method is qualitatively similar to, though simpler than, the EOF-based index described in Wallace et al. (1993). This index is calculated as

$$QBO_i = \frac{1}{\pi} \tan^{-1}\left(\frac{U_{50}}{U_{30}}\right) , \tag{5}$$

and thus ranges from -1 to +1, increasing in time until it reaches +1 and then restarting at -1. QBO_i values between -1 and 0 broadly signify the transition period from easterlies to westerlies throughout the stratosphere, while values between 0 and +1 broadly signify the westerly to easterly transition. By firstly smoothing the zonal winds at both levels with a 31-day boxcar window, this produces a nearly monotonic, cyclic index of the state of the QBO. For this study, we use zonal wind data from ERAi and we split this index into 8 phases with steps of 0.25.

Fig. 7 shows the composite zonal mean zonal wind about this phasing index in gray contours. This composite structure aptly reproduces the expected zonal wind structure of the QBO. For the given 11 years of data, there are four full cycles~~ranging~~, defined here as QBO_i -1 to +1. These four cycles range in length from ~~23.7~~ 24.0 months to ~~33.2~~ 33.7 months, with a mean length of ~~26.9~~ 27.3 months. The means and standard errors of the residence time for each bin is given in Table 1. The range and mean here are well within the observed values (e.g. Baldwin et al., 2001), indicating that this is an appropriate index onto which to composite our calculated momentum fluxes.

The composite ~~8-20 day~~ momentum flux fields are also shown in Fig. 7. The ~~5-20 day composite contains numerous missing data points within~~ largest Kelvin wave momentum flux occurs in the core of the ~~strongest easterlies . These missing data arise from consistently missing data in the 5-8 day period bands for these altitudes and values of QBO_i. The same structure, sans~~

missing data, is captured by the 8-20 day momentum fluxes. Furthermore, the 8-20 day fluxes comprise on average ~60% of the 5-20 day flux amplitudes during easterly QBO phases. Thus we show the 8-20 day composite for ease of analysis.

The largest Kelvin wave momentum fluxes occur during the easterlies while the largest vertical gradient in the flux occurs during the transition from easterlies to westerlies, as expected (Holton and Lindzen, 1972). These maxima track downwards with the transition until the lowermost stratospheric wind is westerly. That this descent occurs primarily during DJFM (Fig. 8) explains why the annual mean climatology displays signals of downward descending fluxes descending signals of the flux and of easterlies during this span. Once the lowermost stratospheric winds are westerly, momentum fluxes become small except within the range of 18-20 km. This is consistent with prior observations of Kelvin waves during westerly QBO phase (Das and Pan, 2013).

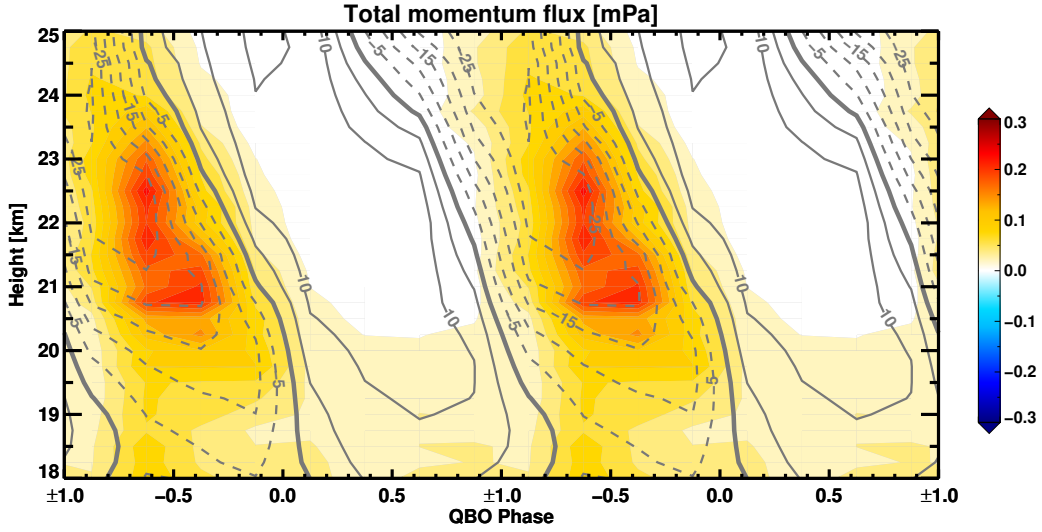

Figure 7. Composite 8-20 day total momentum flux in shading and composite zonal mean zonal winds in gray contours, both as functions of QBO_i (see text for details). Zonal wind contour spacing is 5 m s^{-1} and the 0 m s^{-1} contour is bolded. Two full cycles of the composite QBO are shown here to ease visual inspection.

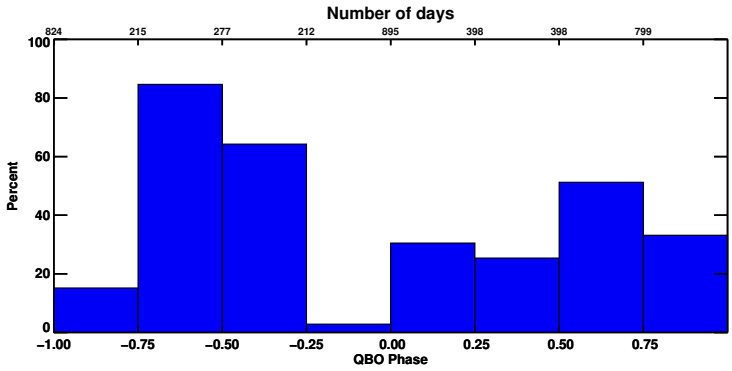

Figure 8. Percent of days in each QBO phase bin that fall between December and March. The total number of days in each bin is given along the top abcissa.

6 Discussion: organized convection and Kelvin waves

A natural step in this line of study is to analyze the relation between tropical convection and our estimated Kelvin wave momentum fluxes. However, tying a certain stratospheric Kelvin wave packet to a specific tropospheric deep convection event is not necessarily straightforward. While Kelvin waves are predominantly generated by convection, not all tropical convection will generate Kelvin waves. When Kelvin waves are forced, their upward propagation will be strongly affected – and often inhibited – by changes in background winds and static stability near the tropical tropopause (e.g., **?**Flannaghan and Fueglistaler, 2012, 2013). Those Kelvin waves that do enter the stratosphere decouple from source convection (Kiladis et al., 2009) making direct attribution difficult without advanced methods for tracking these wave packets.

Rather than relying on advanced techniques to thoroughly quantify the effects of tropical deep convection on stratospheric Kelvin waves, here we show a cursory analysis of this relationship through use of compositing (superposed epoch analysis). Compositing relies on an appropriate definition of an event start date in order to filter out noise in the data, leaving the desired signal. Fundamentally, this method shows the lead-lag relationship between two fields: in our case between a measure of deep convective activity and stratospheric Kelvin waves.

Selecting an event in tropical convection is not straightforward since it is a nearly ubiquitous feature there. However, tropical deep convection is not simply spatially and temporally stochastic, but instead routinely organizes into large-scale patterns, most notably the Madden Julian Oscillation (MJO, Zhang, 2005). And since Kelvin waves project onto the largest scales – zonal wavenumber 1-3 and periods longer than 5 days (Feng et al., 2007; **?**) – a criterion that accounts for the large-scale organization of convection would be appropriate.

Here we define an event as any continuous span of days during which outgoing longwave radiation (OLR) indicative of deep convection covers more than 66% of the upstream area for a given sounding site. We use 200 W/m^2 as our indicator of deep convection in OLR; 180 W/m^2 was also used and found to not result in qualitative changes to the results. The 66% coverage

threshold represents the 90th percentile value of coverage for our reference upstream area. The reference upstream area – taken here to be the 30° longitude west of and ±2.5° latitude around each location – is analyzed because our estimated momentum fluxes are strongly influenced by the environment near to the sounding site (see Section 4). We note that the following results qualitatively hold for other configurations of the upstream area, including if all points between 10°S-10°N are used, so long as the coverage threshold is set to be the 90th percentile value for the considered upstream area. Individual events last for as long as the coverage threshold is continuously met or exceeded. Since the threshold is set to a high level, we do not require a minimum duration. To better isolate the Kelvin wave signals, we do require events to be separated by at least 10 days. Longer separation lengths lead to substantially fewer identified events, but the results qualitatively hold.

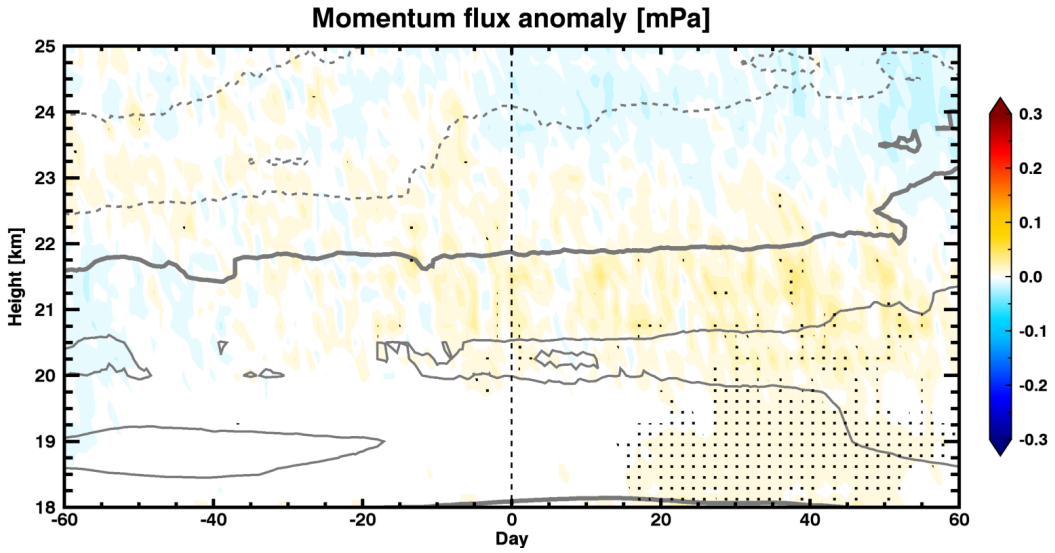

Figure 9. Composite momentum flux anomaly for events where OLR is less than 200 W/m^2 over at least 66% of the reference upsteam area for Manus Island. Day 0 (dashed black line) is the first day this condition is satisfied. The anomaly is the difference from the mean over the entire data record. Stippling indicates where the anomaly is significant at the 95% level. Gray curves are the composite zonal mean zonal wind at 2.5 m s^{-1} spacing, with the 0 m s^{-1} contour bolded. See the text for more details.

Using these event identification criteria, we find 88 events for the Manus sounding site. The composite Kelvin wave momentum flux anomaly and zonal wind are shown in Fig. 9. The anomaly is the difference from the time mean over all points. To evaluate the significance at the 95% level of our composite values, we use a 10000-member Monte Carlo simulation to calculate the confidence interval of a background (randomly selected) composite (**?**). There is a significant signal of positive flux into the lowermost stratosphere in the 20-50 day range following our events. The amplitude of this positive flux represents a ~0.50-0.75 standard deviation anomaly. A similar pattern of variability is found in lag regressions between momentum flux and our convective coverage data (not shown), though the correlations are at most 0.3.

The relatively small amplitudes of the anomalies and low linear correlations indicate that spatially-dense signals in OLR are not the primary factor preceding positive anomalies of momentum flux in the stratosphere. For instance, this composite analysis does not account for the background wind state or changes in stratification, and is only for a single radiosonde site that may miss some or all of the momentum flux signal generated by the local convection. Yet, the 95% significant signal shown here is in line with expectations from theory: organized convection leads to generation of Kelvin waves. These results are also in line with those from Randel and Wu (2005), who showed the broad relationship between Indonesian OLR and lower stratospheric Kelvin wave temperature variance.

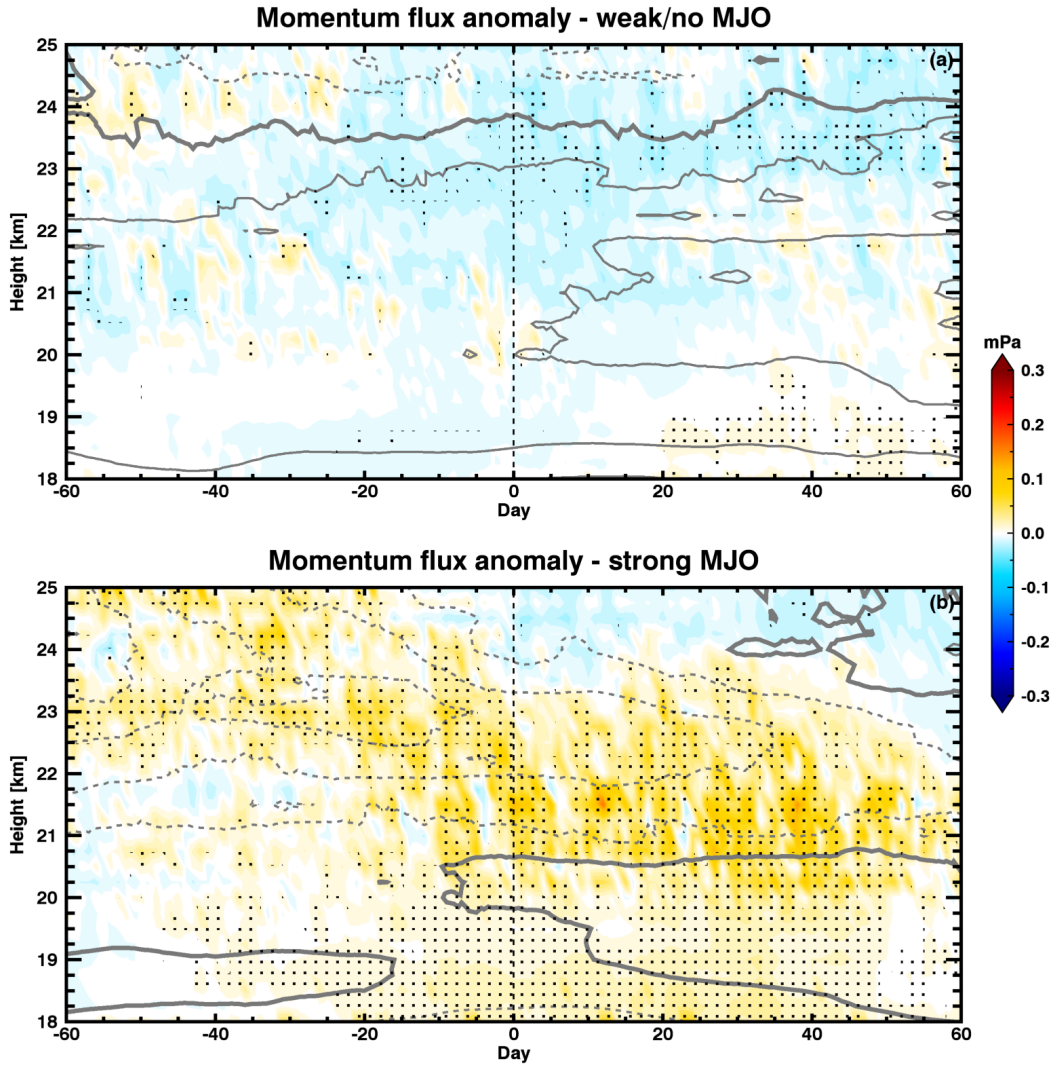

Figure 10. As in Fig. 9, but for subsets of events from those used in Fig. 9 that are (a) weakly associated with the MJO and (b) strongly associated with the MJO.

As noted earlier, such patterns of organized convection in the Tropics are often associated with the convectively active phases of the MJO – phases 3-6 from Wheeler and Hendon (2004). Since the MJO represents the dominant intraseasonal variation of tropical convection and since the MJO has been shown to project Kelvin wave-like temperature structures into the stratosphere (e.g. **?**), we extend this analysis of convection-momentum flux linkage by seeking to determine what impact the MJO has on the lower stratospheric momentum flux. We do so by partitioning our selected events into terciles based on the OLR MJO Index (OMI) values within $\pm$5 days of the event date, the lower and upper thirds representing events that are weakly and strongly

associated with the MJO, respectively. Of the 29 weakly associated events, 14 do not have OMI values above 1 (active MJO) within ± 5 days. In contrast, 27 of the 29 strongly associated events have OMI values above 2 (strongly active MJO) over the same span. Furthermore, 23 of the 29 strongly associated events fall within the convectively active MJO phases 3-6. We are therefore confident that the OLR values used to identify the convective events that are also strongly associated with the MJO are being strongly affected by the active MJO.

Fig. 10 shows the composite momentum flux and zonal wind for both of these subsets of events. Both sets have significant positive anomalies in the 20-50 day range, in line with prior work showing that there is considerable Kelvin wave activity during MJO inactive periods (Virts 2014). However, the anomalies during events strongly associated with the MJO are much larger. The positive anomalies during these events begin prior to the event date, likely due to generation of flux by incipent convection upstream of the sounding site. As stated above, these results hold even if the whole of the Tropics is considered for determination of events so this is not a case of convection not yet entering the reference upstream area. It is likely that the convection that is forcing positive Kelvin wave momentum flux anomalies has not yet grown to cover a large enough area to exceed our threshold.

A second feature of Fig. 10 is the existence of significant positive anomalies above 20 km. These anomalies track downwards in time as the composite zonal wind increases, indicating that these flux anomalies are associated with the easterly phase of the QBO. Son et al. (2017) show that there is a discernable linkage between the phase of the QBO and the amplitude of the MJO, with stronger MJO in easterly QBO. Though these results may be a reflection of that linkage, our compositing does not allow for this kind of definitive attribution. It is not clear if these anomalies are resultant from the upstream convection and thus are tied to the MJO, if they are forced elsewhere and are able to propagate through the favorable mean state, or if they result from aliasing of the QBO into these composites. Methods to calculate anomalies of momentum flux with respect to the QBO would likely lead to a clearer composite signal, but doing so here would be dubious given that only four full QBO cycles are contained in these data.

Our method of compositing with this 11-year record of data is ultimately not sufficient to make definitive arguments about the impact of the MJO on lowermost stratospheric Kelvin wave momentum flux. Nevertheless, the above findings do suggest that the MJO is associated with anomalous increases in the flux, in at least the lowermost stratosphere.

7 Summary

We expand on prior methods for using high-resolution radiosonde observations to estimate upward fluxes of zonal momentum by Kelvin waves. Our methodology~~in particular allows for generation of continuous~~ , in contrast to previous studies that used non-overlapping windows of data, makes use of short-time Fourier transform to generate daily time series of momentum fluxes ~~which~~ that are useful for detailed ~~attribution and climatological analyses .~~ analyses of intraseasonal and interannual variability. Unlike prior work using similar methods, we make use of relatively long-term sources of high-vertical resolution radiosonde data provided by the DOE ARM program to enable analysis of such variability. The qualitative nature of ~~these time series are~~ our derived time series is found to agree well with previous results – e.g. they show amplification during both JFM and QBO

easterly phases – and they qualitatively match prior estimates (cf. Ern and Preusse, 2009, and references therein) though with slightly ~~reduced~~ different amplitudes.

Dependence of our results on vertical and temporal resolution is determined by reprocessing raw radiosonde data across different resolutions and comparing spatially and temporally overlapping points from our momentum flux calculation. Temporal resolution does not strongly affect the flux amplitudes for the tested time steps. In contrast, there is an approximately linear increase in the calculated flux amplitudes ~~for linear increases in the vertical resolution~~with increased vertical step, particularly beyond 500 m resolution (Fig. 2). The root of this relationship comes from our method of estimating the vertical wavelength L_z. For lower vertical resolution, less vertical structure is obtained and the calculation tends towards larger estimates of the vertical wavelength. These longer vertical wavelengths result in smaller values of wavenumbers k and m, though the effect on m is larger because it varies proportionally with L_z (cf. Eq. (4)). From Eqs. (1) and (3), it is clear this will result in larger momentum fluxes ~~.~~for westerly background wind. From Fig. 6, the mean background wind in our data is westerly and thus our resolution tests show increases in momentum flux. In easterly background wind – where the Kelvin wave amplitudes are large – overestimation of the vertical length scales will result in smaller measured flux, underestimating the impact of the Kelvin waves.

Sensitivity to vertical stepping larger than 500 m highlights the need for continued collection of high vertical resolution observations in the tropical stratosphere. Both satellite observations and reanalysis reconstructions have much larger (order 1 km and larger) vertical stepping at these altitudes, so estimations derived from these sources alone may not fully capture the vertical structure. ~~The impact of this may be seen by the larger momentum flux amplitudes derived from these sources~~Perhaps more problematic is that the effect of coarse vertical resolution is not single-signed. Estimates will be too large in westerlies when the flux should be small and will be too small in easterlies when the flux should be large. Advances in remote sensing and computing capabilities will allow for smaller vertical stepping in both these platforms, helping to alleviate this sensitivity. However, there will still be a significant role for routine, high resolution radiosonde data in constraining satellite observations and in nudging data assimilation procedures for reanalyses.

By comparing calculated fluxes from highly-processed radiosonde data during the DYNAMO field campaign to calculated fluxes from synchronous raw radiosonde data at identical and nearby sounding stations, we find that our method is well-suited for application to these raw data, of which there is a considerably longer data record. Kelvin wave momentum fluxes are then calculated from an 11 year span (2003-2013) of quality radiosonde observations from this data record. The annual mean cycle of momentum fluxes shows an annual periodicity with a JFM maximum and a minimum six months later for July through September (Fig. 6). The QBO mean momentum fluxes are large during easterly phase and small during westerly phase (Fig. 7), as expected.

~~There is an important interpretation of the above results that arises when comparing simultaneous calculations of momentum fluxes at different sounding sites (see Figs. 3 and 4): our technique for calculating zonal mean momentum fluxes is strongly influenced by the local contribution to the zonal mean. For the DYNAMO data, Gan Island observations occur within the Indian Ocean where strong convection associated with the MJO is common. The expansive convection associated with these MJO events experienced at Gan Island propagates eastward to Manus Island, but is diminished after propagating over the~~

Maritime Continent (Zhang, 2005). One would expect that such a disruption to the convection will lead to a disruption in the generation of Kelvin waves. This may, in part, explain why the estimated momentum flux amplitudes are smaller at Manus Island, located to the east of the Maritime Continent. Fluxes at Nauru, A composite analysis of events featuring broad deep convection shows that momentum fluxes are significantly increased by 30 days following the onset. Though the signal is only significant up to ∼20 ° to the east of Manus, are similarly smaller (see Figs. S1 and S2). km, the amplitude of the flux increases by ∼0.5-0.75 standard deviations in this region. By binning these events by OMI values and compositing, the data suggest that the MJO significantly increases the momentum flux relative to periods without an active MJO. Further study is necessary to more fully demonstrate the quantitative impact of the MJO.

Our calculated momentum fluxes largely represent local contributions to the zonal mean. However, stratospheric Kelvin waves are known to strongly project onto plantery scales (i.e. zonal wavenumbers 1-3, Feng et al., 2007). This projection may be in part from a quasi-stationary source of these waves: frequent convection over the Indian Ocean and Maritime Continent. It is possible that data from Indian Ocean sounding sites routinely sample the ridges of these planetary-scale, zonal mean momentum fluxes. Our results may then give an upper estimate of the Kelvin wave momentum flux amplitudes. Future, more detailed analyses may reveal more insights into this issue.

A natural step in this line of study is attribution of convective signals to enhanced lower stratospheric Kelvin wave momentum fluxes. We investigated the influence of the MJO, i.e. the dominant intraseasonal pattern in tropical convection, in determining the amplitudes and temporal structure of the derived climatologies.

(left) Mean momentum flux during MJO active periods (solid) and the entire data record (dashed). MJO active periods are where OMI index is greater than 1 for at least 40 days (16 total events). (right) T-statistics for the difference of means between MJO active periods and the total record. Values outside of the gray shading are significant at the 95% level.

The left panel of Fig. 10 shows the mean momentum flux for MJO active periods (solid). MJO active periods are typically defined where the OMI amplitude is at least 1. Here, to ensure that our MJO active period composite does not alias data from inactive periods (OMI amplitude < 1), we require that all days in a given data window must have OMI amplitude ≥ 1. While such points are infrequent (15 distinct events in our data record), they are more likely to have a strong wave signal that projects onto our analyzed periods. We then compare this composite to the entire record (dashed) so as to analyze if the MJO is significantly different from the record mean. Using a comparable separation for MJO inactive period – all days in a given window must have OMI amplitude < 1 – results in relatively few data points.

Though the momentum fluxes in the lowermost stratosphere are larger during MJO active periods , they are not statistically significantly different at the 95% level (right panel). Composite momentum fluxes between 18.5 and 19.5 km are significantly different only at the 85% significance level. This lower stratospheric difference between MJO active periods and the mean state is considerably lower at Nauru Island, further lowering confidence in these results. Furthermore, while the 23 km peak approaches the same level of significant difference, it is well removed from the signal in the lowermost stratosphere. This separation from the source region for Kelvin waves indicates that it is a possible spurious difference. That the above differences are not significant is consistent with previous studies, e.g. Virts and Wallace (2014), that show that MJOinactive periods have considerable Kelvin wave activity in the lower stratosphere.

~~The MJO amplitude is known to have a seasonal cycle that reaches its maximum during DJF (Zhang, 2005), so we analyzed to what degree the MJO affects the JFM maximum of momentum flux (Fig. 6). While the fluxes during MJOactive times are larger than those during inactive times (not shown), the differences are not significant at a meaningful significance level. An analogous separation of the QBO composite into MJO active and inactive times (not shown) finds that the lowermost stratospheric momentum fluxes are larger when the MJO is active, though the results are again not statistically significant.~~

~~However, finding significance with such a statistical analysis is complicated by both the techniques and data used here. The 40 day windowing we use effectively applies a smoothing on the data that is of the order of the typical MJO periodicity of 30-90 days. Thus zonal wind and temperature data points from both inactive and active times are blended together for some calculated momentum flux data points. As shown by Fig. 10, comparing only those data points that fall within MJO active spans of 40 days or longer with data points that fall completely outside of MJO active spans does not change the significance result.~~

~~Doing so in fact only exacerbates an additional complication from the relatively short record length of data. Only 15 events are used in Fig. 10. In our comparison of annual cycles between MJO active and inactive periods, the median number of data points used for each day are seven and four, respectively. For any statistical tests we may apply, the degrees of freedom are small enough that the differences in the composites would need to be dramatic for significance. The differences in QBO composites (not shown) would need to be yet larger since there are only four observed cycles in this data record. Our investigation of MJO influence thus leaves us only with the suggestion of a nontrivial increase in fluxes from enhanced convection during MJO active times, but further study is needed.~~

Such studies should continue technique developments and data analyses that are necessary to further constrain the tropical stratospheric momentum flux budget. Techniques could be developed to incorporate simultaneous soundings from multiple sites into a single calculation of momentum fluxes. The results derived here come from two radiosonde sites, but many additional sites with long data records are available. A careful reprocessing of these radiosonde data may allow for extending the data record with already available data.

Continued collection of high-quality radiosonde observations that probe the tropical stratosphere will also be vital for increasing the number of observed annual and QBO cycles. In addition to the role radiosondes have in forecasting (e.g. Cardinali and Healy, 2014) and climatological studies (e.g. Seidel et al., 2012), recently observed anomalous evolution of the QBO (Newman et al., 2016) further bears out the need for continued radiosonde observations. Additional observations in this region will allow for more robust attribution of wave sources – whether Kelvin, Rossby, or gravity waves – to changes in zonal wind structure in the tropical stratosphere.

Competing interests. The authors declare that they have no conflict of interest.

Acknowledgements. The authors would like to acknowledge Paul Ciesielski for his help in obtaining the L4 DYNAMO data and the raw radiosonde data. The analysis of Section 6 benefited from discussions with Zhen Zeng. We would also like to thank two anonymous

reviewers who provided many helpful comments during the revision of this manuscript. This research was supported by Department of Energy Atmospheric System Research Grant DE-SC0008582.

References

Andrews, D. G., Holton, J. R., and Leovy, C. B.: Middle Atmosphere Dynamics, Academic Press, 1987.

Baldwin, M. P., Gray, L. J., Dunkerton, T. J., Hamilton, K., Haynes, P. H., Randel, W. J., Holton, J. R., Alexander, M. J., Hirota, I., Horinouchi, T., Jones, D. B. A., Kinnersley, J. S., Marquardt, C., Sato, K., and Takahashi, M.: The quasi-biennial oscillation, Rev. Geophys., 39, 179–229, doi:8755-1209/01/1999RG000073, 2001.

Cardinali, C. and Healy, S.: Impact of GPS radio occultation measurements in the ECMWF system using adjoint-based diagnostics, Q. J. R. Meteorol. Soc., 140, 2315–2320, doi:10.1002/qj.2300, 2014.

Ciesielski, P. E., Yu, H., Johnson, R. H., Yoneyama, K., Katsumata, M., Long, C. N., Wang, J., Loehrer, S. M., Young, K., Williams, S. F., Brown, W., Braun, J., and Van Hove, T.: Quality-controlled upper-air sounding dataset for DYNAMO/CINDY/AMIE: development and corrections, J. Atmos. Oceanic Technol., 31, 741–764, doi:10.1175/JTECH-D-13-00165.1, 2014.

Collimore, C. C., Martin, D. W., Hitchman, M. H., Huesman, A., and Waliser, D. E.: On The relationship between the QBO and tropical deep convection, J. Climate, 16, 2552–2568, doi:10.1175/1520-0442(2003)016<2552:OTRBTQ>2.0.CO;2, 2003.

Das, U. and Pan, C. J.: Strong Kelvin wave activity observed during the westerly phase of QBO – a case study, Ann. Geophys., 31, 581–590, doi:10.5194/angeo-31-581-2013, 2013.

Dee, D. P., Uppala, S. M., Simmons, A. J., Berrisford, P., Poli, P., Kobayashi, S., Andrae, U., Balmaseda, M. A., Balsamo, G., Bauer, P., Bechtold, P., Beljaars, A. C. M., van de Berg, L., Bidlot, J., Bormann, N., Delsol, C., Dragani, R., Fuentes, M., Geer, A. J., Haimberger, L., Healy, S. B., Hersbach, H., Holm, E. V., Isaksen, L., Kallberg, P., Kohler, M., Matricardi, M., McNally, A. P., Morcrette, B. M. M.-S. J.-J., Park, B.-K., Puebey, C., de Rosnay, P., Tavolato, C., Thepaut, J.-N., and Vitart, F.: The ERA-Interim reanalysis: configuration and performance of the data assimiliation system, Q. J. R. Meterol. Soc., 137, 553–597, doi:10.1002/qj.828, 2011.

Ern, M. and Preusse, P.: Wave fluxes of equatorial Kelvin waves and QBO zonal wind forcing derived from SABER and ECMWF temperature space-time spectra, Atmos. Chem. Phys., 9, 3957–3986, doi:10.5194/acp-9-3957-2009, 2009.

Feng, L., Harwood, R. S., Brugge, R., O'Neill, A., Froidevaux, L., Schwartz, M., and Waters, J. W.: Equatorial Kelvin waves as revealed by EOS Microwave Limb Sounder observations and European Centre for Medium-Range Weather Forecasts analyses: evidence for slow Kelvin waves of zonal wave number 3, J. Geophys. Res., 112, D16 106, doi:10.1029/2006JD008329, 2007.

Feng, Z., McFarlane, S. A., Schumacher, C., Ellis, S., Comstock, J., and Bharadwaj, N.: Constructing a merged cloud-precipitation radar dataset for tropical convective clouds during the DYNAMO/AMIE experiment at Addu Atoll, J. Atmos. Oceanic Technol., 31, 1021–1042, doi:10.1175/JTECH-D-13-00132.1, 2014.

Flannaghan, T. J. and Fueglistaler, S.: Tracking Kelvin waves from the equatorial troposphere into the stratosphere, J. Geophys. Res., 117, D21 108, doi:10.1029/2012JD017448, 2012.

Flannaghan, T. J. and Fueglistaler, S.: Vertical mixing and the temperature and wind structure of the tropical tropopause layer, J. Atmos. Sci., 71, 1609–1622, doi:10.1175/JAS-D-13-0321.1, 2013.

Fueglistaler, S. and Haynes, P. H.: Control of interannual and longer-term variability of stratospheric water vapor, J. Geophys. Res., 110, D24 108, doi:10.1029/2005JD006019, 2005.

Garfinkel, C. I., Shaw, T. A., Hartmann, D. L., and Waugh, D. W.: Does the Holton–Tan mechanism explain how the quasi-biennial oscillation modulates the arctic polar vortex?, J. Atmos. Sci., 69, 1713–1733, doi:10.1175/JAS-D-11-0209.1, 2012.

Gill, A. E.: Atmosphere-Ocean Dynamics, Academic Press, 1982.

Grise, K. M., Thompson, D. W. J., and Birner, T.: A global survey of static stability in the stratosphere and upper troposphere, J. Climate, 23, 2275–2292, doi:10.1175/2009JCLI3369.1, 2010.

Hitchman, M. H. and Leovy, C. B.: Estimation of the Kelvin wave contribution to the semiannual osccilation, J. Atmos. Sci., 45, 1462–1475, doi:10.1175/1520-0469(1988)045<1462:EOTKWC>2.0.CO;2, 1988.

Holton, J. R. and Lindzen, R. S.: An updated theory for the quasi-biennial cycle of the tropical stratosphere, J. Atmos. Sci., 29, 1076–1080, doi:10.1175/1520-0469(1972)029<1076:AUTFTQ>2.0.CO;2, 1972.

Holton, J. R., Alexander, M. J., and Boehm, M. T.: Evidence for short vertical wavelength Kelvin waves in the Department of Energy-Atmospheric Radiation Measurement Nauru99 radiosonde data, J. Geophys. Res., 106, 20,125–20,129, doi:10.1029/2001JD900108, 2001.

Kiladis, G. N., Wheeler, M. C., Haertel, P. T., Straub, K. H., and Roundy, P. E.: Convectively coupled equatorial waves, Rev. Geophys., 47, RG2003, doi:10.1029/2008RG000266, 2009.

Kiladis, G. N., Dias, J., Straub, K. H., Wheeler, M. C., Tulich, S. N., Kikuchi, K., Weickmann, K. M., and Ventrice, M. J.: A comparison of OLR and circulation-based indices for tracking the MJO, Mon. Wea. Rev., 142, 1697–1715, doi:10.1175/MWR-D-13-00301.1, 2014.

Kim, Y.-H. and Chun, H.-Y.: Momentum forcing of the quasi-biennial oscillation by equatorial waves in recent reanalyses, Atmos. Chem. Phys., 15, 6577–6587, doi:10.5194/acp-15-6577-2015, 2015.

Maruyama, T.: Upward transport of westerly momentum due to large-scale disturbances in the equatorial lower stratosphere, J. Met. Soc. Japan, 46, 404–417, 1968.

Maruyama, T.: Upward transport of westerly momentum due to disturbances of the equatorial lower stratosphere in the period range of about 2 days – a Singapore data analysis for 1983-1993, J. Met. Soc. Japan, 72, 423–432, 1994.

Mather, J. H. and Voyles, J. W.: The ARM climate research facility, Bull. Amer. Meteor. Soc., 94, 377–392, doi:10.1175/BAMS-D-11-00218.1, 2013.

Newman, P. A., Coy, L., Pawson, S., and Lait, L. R.: The anomalous change in the QBO in 2015–2016, Geophys. Res. Lett., 43, doi:10.1002/2016GL070373, 2016.

Randel, W. J. and Wu, F.: Isolation of the ozone QBO in SAGE II data by singular-value decomposition, J. Atmos. Sci., 53, 2546–2559, doi:10.1175/1520-0469(1996)053<2546:IOTOQI>2.0.CO;2, 1996.

Randel, W. J. and Wu, F.: Kelvin wave variability near the equatorial tropopause observed in GPS radio occulation measurements, J. Geophys. Res., 110, D03 102, doi:10.1029/2004JD005006, 2005.

Sato, K. and Dunkerton, T. J.: Estimates of momentum flux associated with equatorial Kelvin and gravity waves, J. Geophys. Res., 102, 26,247–26,261, doi:10.1029/96JD02514, 1997.

Sato, K., Hasegawa, F., and Hirota, I.: Short-period disturbances in the equatorial lower stratosphere, J. Met. Soc. Japan, 72, 859–872, 1994.

Seidel, D. J., Free, M., and Wang, J. S.: Reexamining the warming in the tropical upper troposphere: models versus radiosonde observations, Geophys. Res. Lett., 39, L22 701, doi:10.1029/2012GL053850, 2012.

Straub, K. H., Kiladis, G. N., and Ciesielski, P. E.: The role of equatorial waves in the onset of the South China Sea summer monsoon and the demise of El Niño during 1998, Dyn. Atmos. Oceans, 42, 216–238, doi:10.1016/j.dynatmoce.2006.02.005, 2006.

Thompson, D. W. J., Baldwin, M. P., and Wallace, J. M.: Stratospheric connection to Northern Hemisphere wintertime weather: implications for prediction, J. Climate, 15, 1421–1428, doi:10.1175/1520-0442(2002)015<1421:SCTNHW>2.0.CO;2, 2002.

Tindall, J. C., Thuburn, J., and Highwood, J.: Equatorial waves in the lower stratosphere. II: annual and interannual variability, Q. J. R. Meteorol. Soc., 132, 195–212, doi:10.1256/qj.04.153, 2006.

Virts, K. S. and Wallace, J. M.: Observations of temperature, wind, cirrus, and trace gases in the tropical tropopause transition layer during the MJO, J. Atmos. Sci., 71, 1143–1157, doi:10.1175/JAS-D-13-0178.1, 2014.

Wallace, J. M., Panetta, R. L., and Estberg, J.: Representation of the equatorial stratospheric quasi-biennial oscillation in EOF phase space, J. Atmos. Sci., 50, 1751–1762, doi:10.1175/1520-0442(1993)006<2063:SASOIA>2.0.CO;2, 1993.

Wheeler, M. and Kiladis, G. N.: Convectively coupled equatorial waves: analysis of clouds and temperature in the wavenumber-frequency domain, J. Atmos. Sci., 56, 374–399, doi:10.1175/1520-0469(1999)056<0374:CCEWAO>2.0.CO;2, 1999.

Wheeler, M. C. and Hendon, H. H.: An all-season real-time multivariate MJO index: development of an index for monitoring and prediction, Mon. Wea. Rev., 132, 1917–1932, doi:10.1175/1520-0493(2004)132<1917:AARMMI>2.0.CO;2, 2004.

Xu, W. and Rutledge, S. A.: Morphology, intensity, and rainfall production of MJO convection: observations from DYNAMO shipborne radar and TRMM, J. Atmos. Sci., 72, 623–640, doi:10.1175/JAS-D-14-0130.1, 2015.

Yoneyama, K., Zhang, C., and Long, C. N.: Tracking pulses of the Madden-Julian Oscillation, Bull. Amer. Soc., 94, 1871–1891, doi:10.1175/BAMS-D-12-00157.1, 2013.

Zhang, C.: Madden-Julian Oscillation, Rev. Geophys., 43, RG2003, doi:10.1029/2004RG000158, 2005.